Mon. Not. R. Astron. Soc. **000**, 1–?? (2008) Printed 26 May 2009 (MN LaTeX style file v2.2)

arXiv:0808.2612v2 [astro-ph] 26 May 2009

Uniformly Rotating Homogeneous and Polytropic Rings in Newtonian Gravity

David Petroff⋆ and Stefan Horatschek†
Theoretisch-Physikalisches Institut, University of Jena, Max-Wien-Platz 1, 07743 Jena, Germany

26 May 2009

ABSTRACT

An analytical method is presented for treating the problem of a uniformly rotating, self-gravitating ring without a central body in Newtonian gravity. The method is based on an expansion about the thin ring limit, where the cross-section of the ring tends to a circle. The iterative scheme developed here is applied to homogeneous rings up to the 20th order and to polytropes with the index $n = 1$ up to the third order. For other polytropic indices no analytic solutions are obtainable, but one can apply the method numerically. However, it is possible to derive a simple formula relating mass to the integrated pressure to leading order without specifying the equation of state. Our results are compared with those generated by highly accurate numerical methods to test their accuracy.

Key words: gravitation – methods: analytical – hydrodynamics – equation of state – stars: rotation.

1 INTRODUCTION

The problem of the self-gravitating ring captured the interest of such renowned scientists as Kowalewsky (1885), Poincaré (1885a,b,c) and Dyson (1892, 1893). Each of them tackled the problem of an axially symmetric, homogeneous ring in equilibrium by expanding it about the thin ring limit. In particular, Dyson provided a solution to fourth order in the parameter $\sigma = a/b$, where a provides a measure for the radius of the cross-section of the ring and b the distance of the cross-section's centre of mass from the axis of rotation. An important step toward understanding rings with other equations of state was taken by Ostriker (1964a,b, 1965), who studied polytropic rings to first order in σ and found a complete solution to this order for an isothermal limit.

First numerical results for homogeneous rings were given by Wong (1974), who was not able to clarify the transition to spheroidal bodies that Bardeen (1971) had supposed would exist. Eriguchi & Sugimoto (1981) and Eriguchi & Hachisu (1985) developed improved methods with which they were able to study the connection to the Maclaurin spheroids. Returning to the problem significantly later, Ansorg, Kleinwächter & Meinel (2003c) achieved near-machine accuracy, which allowed them to study bifurcation sequences in detail and correct erroneous results. It was also possible to extend the problem to non-homogeneous rings and even to the framework of General Relativity (Hachisu 1986; Ansorg, Kleinwächter & Meinel 2003b; Fischer, Horatschek & Ansorg 2005).

Through the use of computer algebra, we extend Dyson's basic idea and determine the solution to the problem of the homogeneous ring up to the order σ^{20}. We also present an iterative method for performing a similar expansion about the thin ring limit for arbitrary equations of state and general results are derived, confirming and generalizing work that had already been published by Ostriker (1964b). The application to polytropes is considered and ordinary differential equations (ODEs) are found that allow for the determination of the mass density. A closed-form solution can only be found if the value of the polytropic index is $n = 1$, and such rings are considered to the order σ^3. For other polytropic indices, the ODEs are solved numerically so that results from the approximate scheme can be compared to highly accurate numerical results for a variety of equations of state. The numerical solutions considered here are taken from a multi-domain spectral program, much like the one described in Ansorg, Kleinwächter & Meinel (2003a), but tailored to Newtonian bodies with toroidal topologies (see Ansorg & Petroff 2005 for more information). The solutions obtained by these numerical methods are extremely accurate and thus provide us with a means of testing the accuracy of the approximate method.

⋆ E-mail: `D.Petroff@tpi.uni-jena.de`
† E-mail: `S.Horatschek@tpi.uni-jena.de`

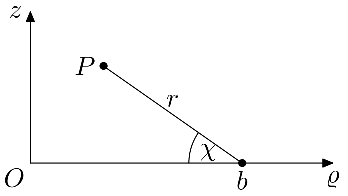

Figure 1. A sketch providing the meaning of the coordinates (r, χ) in relation to the cylindrical coordinates (ϱ, z).

2 THE APPROXIMATION SCHEME

2.1 The Coordinates

To describe axially symmetric rings, we introduce the polar-like coordinates (r, χ, φ), which are related to the cylindrical coordinates (ϱ, z, φ) by

$$\varrho = b - r\cos\chi, \quad z = r\sin\chi, \quad \varphi = \varphi. \tag{1}$$

For a given value of φ, constant values of the coordinate r are circles centred about $(\varrho = b, z = 0)$ and χ measures the angle along any such circle. Fig. 1 provides an illustration of the coordinates. The surface of the ring will be described by a function $r_\mathrm{s}(\chi)$. In our coordinates, the Laplace operator applied to a function $f = f(r, \chi)$ reads

$$\begin{aligned}\nabla^2 f =& \frac{\partial^2 f}{\partial r^2} + \frac{1}{r}\frac{\partial f}{\partial r} + \frac{1}{r^2}\frac{\partial^2 f}{\partial \chi^2} \\ & - (b - r\cos\chi)^{-1}\left(\cos\chi\frac{\partial f}{\partial r} - \frac{\sin\chi}{r}\frac{\partial f}{\partial \chi}\right).\end{aligned} \tag{2}$$

We choose the constant b in such a manner that the centre of mass of the ring's cross-section coincide with $r = 0$, thus implying

$$\int_0^{2\pi}\int_0^{r_\mathrm{s}(\chi)} \mu r^2 \cos\chi \,\mathrm{d}r\,\mathrm{d}\chi = 0, \tag{3}$$

where μ is the mass density.

2.2 Basic Equations

For solving the problem of a self-gravitating fluid in equilibrium, we have to fulfil Laplace's equation

$$\nabla^2 U_\mathrm{out} = 0 \tag{4}$$

outside the fluid and Poisson's equation

$$\nabla^2 U_\mathrm{in} = 4\pi G\mu \tag{5}$$

inside it, where U is the gravitational potential. Additionally, we have to satisfy Euler's equation

$$\mu\frac{\mathrm{d}\boldsymbol{v}}{\mathrm{d}t} = -\mu\nabla U_\mathrm{in} - \nabla p, \tag{6}$$

where $\boldsymbol{v}$ is the velocity of a fluid element and p the pressure. We consider uniform rotation about the axis $\varrho = 0$ with the angular velocity $\boldsymbol{\Omega}$ and thus have the velocity field

$$\boldsymbol{v} = \boldsymbol{\Omega} \times \boldsymbol{x} \tag{7}$$

leading to

$$\nabla\left(U_\mathrm{in} + \int_0^p \frac{\mathrm{d}p'}{\mu(p')} - \frac{1}{2}\Omega^2\varrho^2\right) = 0. \tag{8}$$

We introduce the pressure function

$$h := \int_0^p \frac{\mathrm{d}p'}{\mu(p')}, \tag{9}$$

which is nothing other than the specific enthalpy in the case of constant specific entropy. Integration gives

$$U_\mathrm{in} + h - \frac{1}{2}\Omega^2\varrho^2 = V_0, \tag{10}$$

where V_0 is the constant of integration. At the surface of the ring, where the pressure vanishes, we have

$$U_\mathrm{s} - \frac{1}{2}\Omega^2\varrho^2\bigg|_\mathrm{s} = V_0. \tag{11}$$

2.3 Series Expansions

The thin ring limit is approached when the ratio of the inner radius ϱ_i to the outer one ϱ_o tends to 1. In this limit, the cross-section of the ring becomes a circle. This is the starting point of the approximation. As an interesting aside, if one considers a ring surrounding a central body, for example a point mass, the cross-section of the ring can deviate significantly from a circle even if the radius ratio is close to 1, see Fig. 8 in Ansorg & Petroff (2005).

We describe the surface of the ring up to order q by the Fourier series

$$r_\mathrm{s}(\chi) = a\left(1 + \sum_{i=1}^{q}\sum_{k=0}^{i}\beta_{ik}\cos(k\chi)\sigma^i + o(\sigma^q)\right), \tag{12}$$

where

$$\sigma := \frac{a}{b}. \tag{13}$$

There are no sine terms because of reflectional symmetry with respect to the equatorial plane, a symmetry necessarily present for fluids in equilibrium (see Lichtenstein 1933). To the leading order, the cross-section is indeed a circle of radius a. We make a similar ansatz for the mass density, pressure function, pressure and the potential inside the ring

$$\mu(r, \chi) = \mu_\mathrm{c}\left(\sum_{i=0}^{q}\sum_{k=0}^{i}\mu_{ik}(y)\cos(k\chi)\sigma^i + o(\sigma^q)\right), \tag{14}$$

$$h(r, \chi) = \pi G\mu_\mathrm{c}a^2\left(\sum_{i=0}^{q}\sum_{k=0}^{i}h_{ik}(y)\cos(k\chi)\sigma^i + o(\sigma^q)\right), \tag{15}$$

$$p(r, \chi) = \pi G\mu_\mathrm{c}^2a^2\left(\sum_{i=0}^{q}\sum_{k=0}^{i}p_{ik}(y)\cos(k\chi)\sigma^i + o(\sigma^q)\right), \tag{16}$$

$$U_\mathrm{in}(r, \chi) = -\pi G\mu_\mathrm{c}a^2\left(\sum_{i=0}^{q}\sum_{k=0}^{i}U_{ik}(y)\cos(k\chi)\sigma^i + o(\sigma^q)\right), \tag{17}$$

where we have introduced the dimensionless radius

$$y := \frac{r}{a}. \tag{18}$$

The quantity μ_c is chosen to be the mass density at the point $r = 0$ and does not represent the density's maximal value, although it will not differ significantly from it in general. For the square of the angular velocity, we write

$$\Omega^2 = \pi G \mu_\mathrm{c} \left(\sum_{i=0}^{q+2} \Omega_i \sigma^i + o(\sigma^{q+2}) \right) \tag{19}$$

and for V_0

$$V_0 = -\pi G \mu_\mathrm{c} a^2 \left(\sum_{i=0}^{q} v_i \sigma^i + o(\sigma^q) \right). \tag{20}$$

Since the potential outside the ring contains logarithmic terms in r it will come as no surprise that there are $\ln \sigma$ terms in the coefficients of our series. Like Dyson, we introduce

$$\lambda := \ln \frac{8}{\sigma} - 2. \tag{21}$$

Because $\lim_{\sigma \to 0} \sigma \lambda^\alpha = 0$ for all α, this dependence will not pose a problem for the iteration scheme.

2.4 Determination of the Coefficients

We now present a method for determining μ_{qk}, Ω_{q+1} and β_{qk} given that the previous terms in σ^i are known.

The idea used in Dyson's approximation scheme for homogeneous rings makes use of the Poisson integral to determine the gravitational potential in terms of the (still unknown) function $r_\mathrm{s}(\chi)$ along the axis of rotation (Dyson 1892). This is only possible since the mass density is completely determined for homogeneous matter once the shape of the ring is given. In general, however, it is necessary first to determine μ to the desired order before being able to perform the integral. By taking the divergence of the Euler equation (8), using (5) and expressing h as a function of μ using the equation of state, we obtain a second order PDE for μ:

$$4\pi G \mu + \nabla^2 h - 2\Omega^2 = 0. \tag{22}$$

Expanding in terms of σ and requiring that the equations be satisfied for each power in σ and each term in the Fourier expansion then results in ODEs for $\mu_{qk}(y)$ once an equation of state has been specified. These functions must be regular at the origin and chosen such that $\mu_{00}(0) = 1$ and $\mu_{ik}(0) = 0$ for all other i and k so as to be consistent with the choice $\mu(0, \chi) = \mu_\mathrm{c}$. For $k = 0$, this condition suffices to determine the function uniquely. For $k = 1, 2, \ldots, q$, the remaining constants in the solutions of the ODEs are found by requiring that the pressure and thus pressure function vanish at the surface. Demanding this for each of the coefficients in a Fourier expansion, provides $q + 1$ equations for the remaining q constants. The additional equation can be used to determine β_{q0}.

Although the Poisson integral is valid everywhere, for technical reasons, we first calculate the potential on the axis of symmetry only. After this, we determine the potential outside the ring and in particular along its surface, where (11) must hold.

We label the coordinates for a point on the axis $(R, \chi_R) \equiv (r, \chi)$, from which

$$b = R \cos(\chi_R) \tag{23}$$

follows. The axis potential is

$$\begin{aligned} U_\mathrm{axis}(R) &= -2\pi G \int_0^{2\pi} \int_0^{r_\mathrm{s}(\chi')} \frac{\mu\,(b - r\cos\chi')r}{\sqrt{R^2 + r^2 - 2Rr\cos\psi}} \,\mathrm{d}r\,\mathrm{d}\chi' \\ &= -2\pi G \int_0^{2\pi} \int_0^{r_\mathrm{s}(\chi')} \mu(b - r\cos\chi') \sum_{l=0}^{\infty} \left(\frac{r}{R}\right)^{l+1} P_l(\cos\psi)\,\mathrm{d}r\,\mathrm{d}\chi' \\ &=: -2\pi^2 G \mu_\mathrm{c} a^2 \sum_{l=1}^{\infty} \frac{(2l-1)!!}{2l-1} \left(\frac{a}{R}\right)^{2l-1} \frac{A_l}{\sigma^l} \\ &= -2\pi^2 G \mu_\mathrm{c} a^2 \left(\sum_{l=1}^{q+1} \frac{(2l-1)!!}{2l-1} \left(\frac{a}{R}\right)^{2l-1} \frac{A_l}{\sigma^l} + o(\sigma^q) \right), \end{aligned} \tag{24}$$

where $\psi := \chi' - \chi_R$ and P_l denote the Legendre polynomials. Please note that the expansion in terms of powers of $1/R$ indicated in the last line is not trivial, since there is an R-dependence hidden in the terms with ψ. Because of reflectional symmetry, there are only terms with odd powers in $1/R$. We expand A_l with respect to σ

$$A_l = \sum_{i=l-1}^{q} \alpha_{li} \sigma^i + o(\sigma^q). \tag{25}$$

Using U_axis, we can then find the potential anywhere in the vacuum region. To do so, we first introduce a set of axially symmetric solutions to Laplace's equation that vanish at infinity. We define

$$I_1(\varrho, z) := \int_0^{\pi} \frac{\mathrm{d}\varphi}{\sqrt{b^2 + \varrho^2 + z^2 - 2b\varrho\cos\varphi}}, \tag{26}$$

which is nothing other than a multiple of the potential of a circular line of mass with radius b, centred around the axis. In (r, χ, φ)-coordinates it reads

$$I_1(r, \chi) = \frac{2K\left(\sqrt{\frac{4b^2 - 4br\cos\chi}{4b^2 - 4br\cos\chi + r^2}}\right)}{\sqrt{4b^2 - 4br\cos\chi + r^2}}, \tag{27}$$

where K denotes the complete elliptic integral of the first kind,

$$K(k) := \int_0^{\frac{\pi}{2}} \frac{\mathrm{d}\theta}{\sqrt{1 - k^2 \sin^2\theta}}. \tag{28}$$

Because the difference of two such solutions with different b's also satisfies Laplace's equation, it is clear that

$$I_l(r, \chi) := \left(-\frac{1}{b}\frac{\mathrm{d}}{\mathrm{d}b}\right)^{l-1} I_1(r, \chi), \tag{29}$$

where

$$\frac{\mathrm{d}}{\mathrm{d}b} = \frac{\partial}{\partial b} + \cos\chi \frac{\partial}{\partial r} - \frac{\sin\chi}{r}\frac{\partial}{\partial \chi}, \tag{30}$$

is also a solution of Laplace's equation. Next we note that along the axis we have

$$I_l(R) = \frac{\pi(2l-1)!!}{(2l-1)R^{2l-1}}. \tag{31}$$

It then follows that the potential in the vacuum region is

$$U_\mathrm{out}(r, \chi) = -2\pi G \mu_\mathrm{c} a^2 \left(\sum_{l=1}^{q+1} a^{2l-1} \sigma^{-l} A_l I_l + o(\sigma^q) \right), \tag{32}$$

since this expression satisfies Laplace's equation, vanishes at infinity and has the correct value along the axis. For calculating the potential at the body's surface we expand $I_l(r,\chi)$ for $r<b$. For example we get

$$I_1(r,\chi) = \frac{1}{b}\left[\ln\left(\frac{8b}{r}\right) + \frac{[\ln(8b/r)-1]\cos\chi}{2}\,\frac{r}{b} + o\left(\frac{r}{b}\right)\right]. \tag{33}$$

After evaluating these equations for $I_l(r,\chi)$ at the surface $r = r_{\mathrm{s}}(\chi)$, we use (32) to find the coefficients ϕ_{ik} in the expansion

$$U_{\mathrm{s}}(\chi) = -2\pi G\mu_{\mathrm{c}}a^2\left(\sum_{i=0}^{q}\sum_{k=0}^{i}\phi_{ik}\cos(k\chi)\sigma^i + o(\sigma^q)\right). \tag{34}$$

The coefficients ϕ_{qk} still depend on q unknown β_{qk} (remember that β_{q0} is already known). By comparing the coefficients of $\cos(k\chi)$ $(k = 1, 2, \ldots, q)$, equation (11) provides q equations. Together with equation (3) to the relevant order in σ, we can solve for Ω_{q+1} and the aforementioned β_{qk}. The absolute term ($\cos(0\chi)$) gives a relation between Ω_{q+2} and v_q.

3 GENERAL RESULTS TO FIRST ORDER

The approximation scheme described above allows us to draw certain conclusions even without specifying the equation of state, thus generalizing results that were published for polytropes by Ostriker (1964b). To leading order in σ, where nothing depends on the angle χ, the ring (here a torus) is equivalent to an infinitely long cylinder, a problem that was studied by Chandrasekhar & Fermi (1953); Ostriker (1964a). Equation (22) now reads

$$\left(\frac{\mathrm{d}^2}{\mathrm{d}y^2} + \frac{1}{y}\frac{\mathrm{d}}{\mathrm{d}y}\right)h_{00} + 4\mu_{00} = 0, \tag{35}$$

since the integrated Euler equation (10) tells us that

$$\frac{\Omega^2}{G\mu_{\mathrm{c}}} = o(\sigma^2) \tag{36}$$

must hold, i.e.

$$\Omega_0 = \Omega_1 = 0. \tag{37}$$

At the surface of the ring $r = r_{\mathrm{s}}$, the pressure vanishes, corresponding to $h(r = r_{\mathrm{s}}) = 0$, and we thus find

$$h_{00}(1) = 0 \tag{38}$$

and

$$\beta_{11} = -h_{11}\left(\frac{\mathrm{d}h_{00}}{\mathrm{d}y}\right)^{-1}\Bigg|_{y=1}. \tag{39}$$

By multiplying (35) by $\pi^2\mu_{\mathrm{c}}a^2by$ and integrating from 0 to 1, one finds that the mass M to leading order can be related to the derivative of h_{00} at the point $y=1$ according to

$$M = 4\pi^2\mu_{\mathrm{c}}a^2b\int_0^1\mu_{00}y\,\mathrm{d}y = -\pi^2\mu_{\mathrm{c}}a^3\sigma^{-1}\left.\frac{\mathrm{d}h_{00}}{\mathrm{d}y}\right|_{y=1}. \tag{40}$$

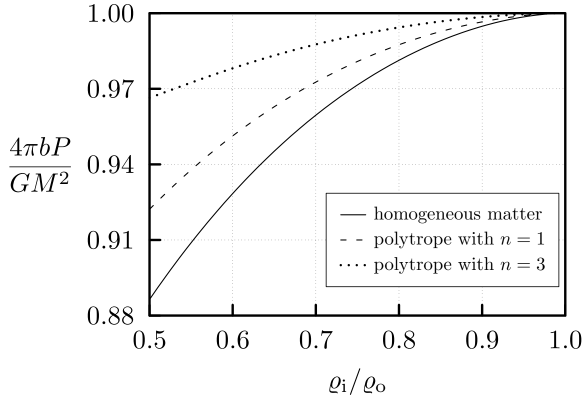

Figure 2. Numerical examples demonstrating how $4\pi bP/GM^2$ tends to 1 in the thin ring limit for various equations of state, cf. equation (42).

A particularly interesting relation involving the square of the mass can be derived by considering the integral over the pressure

$$P := 2\pi\int_0^{2\pi}\int_0^{r_{\mathrm{s}}(\chi)} pr(b - r\cos\chi)\,\mathrm{d}r\,\mathrm{d}\chi. \tag{41}$$

To leading order, upon taking (35) into account, this integral reads

$$\begin{aligned}
P &= 4\pi^3G\mu_{\mathrm{c}}^2a^4b\int_0^1 p_{00}y\,\mathrm{d}y\\
&= -2\pi^3G\mu_{\mathrm{c}}^2a^4b\int_0^1\frac{\mathrm{d}p_{00}}{\mathrm{d}y}y^2\,\mathrm{d}y\\
&= -2\pi^3G\mu_{\mathrm{c}}^2a^4b\int_0^1\mu_{00}\frac{\mathrm{d}h_{00}}{\mathrm{d}y}y^2\,\mathrm{d}y\\
&= 8\pi^3G\mu_{\mathrm{c}}^2a^4b\int_0^1\mu_{00}y\left(\int_0^y\mu_{00}y'\,\mathrm{d}y'\right)\mathrm{d}y\\
&= 4\pi^3G\mu_{\mathrm{c}}^2a^4b\left(\int_0^1\mu_{00}y\,\mathrm{d}y\right)^2\\
&= \frac{GM^2}{4\pi b}.
\end{aligned} \tag{42}$$

Numerical examples demonstrating how $4\pi bP/GM^2$ approaches 1 in the thin ring limit for various equations of state can be found in Fig. 2.

Equation (3) tells us that

$$\beta_{11}\mu_{00}(1) + \int_0^1\mu_{11}y^2\,\mathrm{d}y = 0 \tag{43}$$

holds. The terms from the expansions (32) and (25) of the potential in the vacuum that we need here are

$$\alpha_{10} = 2\int_0^1\mu_{00}y\,\mathrm{d}y = \frac{M\sigma}{2\pi^2\mu_{\mathrm{c}}a^3} \tag{44}$$

and

$$\alpha_{21} = \frac{gM\sigma}{2\pi^2\mu_{\mathrm{c}}a^3}, \qquad g := -\frac{\pi^2\mu_{\mathrm{c}}a^3}{M\sigma}\int\limits_0^1 \mu_{00}y^3\,\mathrm{d}y, \tag{45}$$

where we used (43). The coefficient Ω_2 from the expansion of the square of the angular velocity follows from the coefficient in front of $\cos(\chi)\sigma$ in (11) and reads

$$\Omega_2 = \alpha_{10}(1+\lambda-2\beta_{11}) + 2\alpha_{21}. \tag{46}$$

According to (32) and (33), the potential at the surface is

$$U_{\mathrm{s}} = -\frac{GM}{\pi b}(\lambda + 2 + o(1)) \tag{47}$$

and the constant of integration V_0 then follows immediately from the leading order of (11)

$$\begin{aligned} V_0 &= \left(U_{\mathrm{out}} - \frac{1}{2}\Omega^2\varrho^2\right)\Bigg|_{r=r_{\mathrm{s}}} \\ &= -\frac{GM}{2\pi b}\left(\frac{5\lambda+9}{2} + g - \beta_{11} + o(1)\right). \end{aligned} \tag{48}$$

The term $g - \beta_{11}$ appearing in the above equation can be treated further by considering the rotational energy T and potential energy W and making use of the virial identity

$$0 = 3P + 2T + W, \tag{49}$$

which then implies

$$0 = 3P + \frac{GM^2}{\pi b}\left(g - \beta_{11} - \frac{1}{2}\right) - 2\pi^3 G\mu_{\mathrm{c}}^2 a^4 b\int\limits_0^1 \mu_{00}h_{00}y\,\mathrm{d}y. \tag{50}$$

By restricting ourselves to the polytropic equation of state (see (88)), we can rewrite the above integral to read

$$\begin{aligned} \int\limits_0^1 \mu_{00}h_{00}y\,\mathrm{d}y &= \frac{(n+1)K\mu_{\mathrm{c}}^{1/n-1}}{\pi G a^2}\int\limits_0^1 \mu_{00}^{1+1/n}y\,\mathrm{d}y \\ &= (n+1)\int\limits_0^1 p_{00}y\,\mathrm{d}y = \frac{(n+1)M^2}{16\pi^4\mu_{\mathrm{c}}^2a^4b^2}, \end{aligned} \tag{51}$$

where the last step follows from (42). Putting this expression into (50) and using (42) again then yields

$$g - \beta_{11} = \frac{n-1}{8}. \tag{52}$$

Taking into account $1 - \varrho_{\mathrm{i}}/\varrho_{\mathrm{o}} = 2\sigma$, which holds to leading order, we can use (46) to write

$$\frac{2\pi b^3\Omega^2}{GM} + \ln\left(1 - \frac{\varrho_{\mathrm{i}}}{\varrho_{\mathrm{o}}}\right) \to \frac{n-5}{4} + \ln 16 \tag{53}$$

and (48) can be written as

$$\frac{4\pi b V_0}{5GM} - \ln\left(1 - \frac{\varrho_{\mathrm{i}}}{\varrho_{\mathrm{o}}}\right) \to \frac{5-n}{20} - \ln 16 \tag{54}$$

for polytropes in the thin ring limit. Similar equations can be derived for J, T, P and via the virial identity for W (see Ostriker 1964b). These equations also hold for homogeneous bodies ($n = 0$) and numerical examples demonstrating the behaviour (54) are provided in Fig. 3.

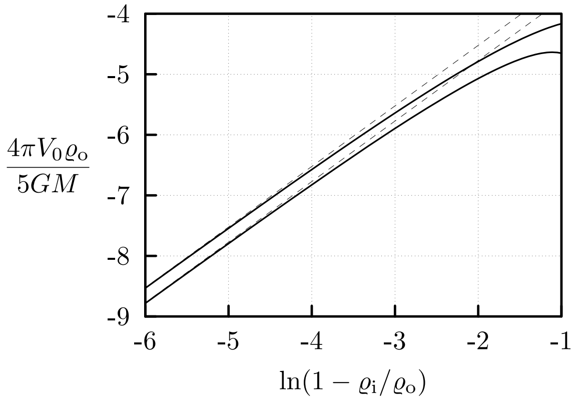

Figure 3. Numerical ring sequences (solid lines) for homogeneous matter (upper curve) and polytropes with $n = 5$ (lower curve) are plotted for rings approaching the thin ring limit. The asymptotic behaviour as given by equation (54) is indicated by the dashed lines.

4 HOMOGENEOUS RINGS

Homogeneous matter is defined by the simple mass distribution

$$\mu = \mu_{\mathrm{c}}, \tag{55}$$

and we can write

$$\mu_{ik} = \begin{cases} 1 & \text{if } i = k = 0 \\ 0 & \text{otherwise} \end{cases}. \tag{56}$$

The integral (9) for the pressure function gives $h = p/\mu_{\mathrm{c}}$, which means that $h_{ik} = p_{ik}$.

For homogeneous rings, it is possible to choose

$$\beta_{i0} = 0 \tag{57}$$

without loss of generality.

4.1 The Zeroth Order: $\boldsymbol{\sigma^0}$

To leading order, the ring is truly a torus

$$r_{\mathrm{s}} = a[1 + o(1)] \tag{58}$$

and equation (3) is thus automatically fulfilled. The potential along the axis is that of a solid torus[1], which can be written down explicitly

$$\begin{aligned} U_{\mathrm{axis}} = -\frac{8\pi G\mu_{\mathrm{c}}a^3}{3R}\Bigg[&\left(1 + \frac{R^2}{a^2}\right)E\left(\frac{a}{R}\right)\sigma^{-1} \\ &+ \left(1 - \frac{R^2}{a^2}\right)K\left(\frac{a}{R}\right)\sigma^{-1} + o(\sigma^{-1})\Bigg]. \end{aligned} \tag{59}$$

An expansion in powers of $1/R$ then gives

$$A_1 = 1 + o(1) \quad\Longrightarrow\quad \alpha_{10} = 1. \tag{60}$$

We can extend this axis potential to the whole exterior of the ring via (32), and expand it on the surface (58) by using (33) in σ. We get

$$U_{\mathrm{s}} = -2\pi G\mu_{\mathrm{c}}a^2\left[\lambda + 2 + o(1)\right], \tag{61}$$

---

[1] E denotes the complete elliptic integral of the second kind, $E(k) := \int_0^{\frac{\pi}{2}}\sqrt{1 - k^2\sin^2\theta}\,\mathrm{d}\theta$.

which implies

$$\phi_{00} = \lambda + 2. \tag{62}$$

Evaluating equation (11) confirms (37) and provides the relation

$$\Omega_2 = 2v_0 - 4(\lambda + 2). \tag{63}$$

This equation cannot be further evaluated until the next order $q = 1$.

To calculate the inner structure, we have to solve equation (35), where the mass density is given by (56). The solution is

$$h_{00} = -y^2 + C_1 \ln y + C_2. \tag{64}$$

At the centre, the pressure function has to be regular, thus $C_1 = 0$, and it must vanish at the surface (38), thus $C_2 = 1$. The integrated Euler equation (10) gives us the potential to this order

$$U_{00} = h_{00} + v_0 - \frac{\Omega_2}{2},$$

where both v_0 and Ω_2 are unknown, but the required combination of them is given by (63) and we can conclude

$$U_{00} = 2\lambda + 5 - y^2,$$

which indeed gives (61) at the surface.

4.2 The First Order: σ^1

The surface function reads

$$r_\mathrm{s} = a[1 + \beta_{11}\sigma\cos\chi + o(\sigma)] \tag{65}$$

and equation (3) becomes

$$0 = \int_0^{2\pi} r_\mathrm{s}^3 \cos\chi \,\mathrm{d}\chi = a^3[3\pi\beta_{11}\sigma + o(\sigma)]. \tag{66}$$

This gives

$$\beta_{11} = 0, \tag{67}$$

cf. (43), which means that we have again the surface function (58), but one step further in σ:

$$r_\mathrm{s} = a[1 + o(\sigma)]. \tag{68}$$

Accordingly, we get the same potential as (59), but with $o(1)$ instead of $o(\sigma^{-1})$. The expansion in terms of powers of $1/R$ gives

$$A_1 = 1 + o(\sigma) \quad\text{and}\quad A_2 = -\frac{\sigma}{8} + o(\sigma). \tag{69}$$

The new coefficients are

$$\alpha_{11} = 0 \quad\text{and}\quad \alpha_{21} = -\frac{1}{8}. \tag{70}$$

Again we are able to calculate the potential at the body's surface (68) via (32), (33) and the corresponding equation for I_2. We get

$$U_\mathrm{s} = -2\pi G\mu_\mathrm{c} a^2 \left[\lambda + 2 + \left(\frac{\lambda}{2} + \frac{3}{8}\right)\sigma\cos\chi + o(\sigma)\right], \tag{71}$$

which gives us the new coefficients

$$\phi_{10} = 0 \quad\text{and}\quad \phi_{11} = \frac{\lambda}{2} + \frac{3}{8}. \tag{72}$$

Plugging the expansion

$$\frac{1}{2}\Omega^2\varrho^2\Big|_\mathrm{s} = \pi G\mu_\mathrm{c} a^2 \left[\frac{\Omega_2}{2} + \left(\frac{\Omega_3}{2} - \Omega_2\cos\chi\right)\sigma + o(\sigma)\right] \tag{73}$$

together with (20) and (71) into (11) yields two new equations when one collects the coefficients in $\sigma^i\cos(k\chi)$:

$$\Omega_2 = \lambda + \frac{3}{4}, \tag{74}$$

$$\Omega_3 = 2v_1. \tag{75}$$

Using equation (63) then gives

$$v_0 = \frac{5}{2}\lambda + \frac{35}{8}. \tag{76}$$

Equation (75) cannot be further evaluated until the next order $q = 2$.

For the mass and the angular momentum, we get

$$M = 2\pi^2\mu_\mathrm{c} a^3[\sigma^{-1} + o(1)] \tag{77}$$

and

$$J = \sqrt{\pi^5 G\mu_\mathrm{c}^3\,(4\lambda + 3)}\, a^5[\sigma^{-2} + o(\sigma^{-2})]. \tag{78}$$

To leading order, $\varrho_\mathrm{i}/\varrho_\mathrm{o} = 1 - 2\sigma$ holds, and we can conclude that

$$\lim_{\varrho_\mathrm{i}/\varrho_\mathrm{o}\to 1}\left[\frac{4\pi b V_0}{5GM} - \ln\left(1 - \frac{\varrho_\mathrm{i}}{\varrho_\mathrm{o}}\right)\right] = \frac{1}{4} - \ln 16, \tag{79}$$

as we already saw in (54), see also equation (11) in Fischer, Horatschek & Ansorg (2005).

To calculate the inner quantities, we have to find a solution to (22). The ansatz (15) leads to the ODEs

$$\frac{\mathrm{d}^2 h_{10}}{\mathrm{d}y^2} + \frac{1}{y}\frac{\mathrm{d}h_{10}}{\mathrm{d}y} = 0 \tag{80}$$

and

$$\frac{\mathrm{d}^2 h_{11}}{\mathrm{d}y^2} + \frac{1}{y}\frac{\mathrm{d}h_{11}}{\mathrm{d}y} - \frac{h_{11}}{y^2} + 2y = 0. \tag{81}$$

Note that the $2y$ term in the second equation results from $h_{00} = 1 - y^2$, which is already known. The solutions of these equations that are regular at the centre and obey $h(r_\mathrm{s}) = 0$ are

$$h_{10} = 0 \tag{82}$$

and

$$h_{11} = \frac{y}{4}(1 - y^2). \tag{83}$$

Using these results, equation (10) then gives

$$U_{10} = 0 \tag{84}$$

and

$$U_{11} = (\lambda + 1)y - \frac{y^3}{4}. \tag{85}$$

After finding the inner potential and pressure, we can calculate the potential energy

$$W = \frac{\mu_\mathrm{c}}{2}\int U\,\mathrm{d}V = -\pi^3 G\mu_\mathrm{c}^2 a^5\left[\left(2\lambda + \frac{9}{2}\right)\sigma^{-1} + o(1)\right],$$

the rotational energy

$$T = \frac{\mu_\mathrm{c}\Omega^2}{2}\int \varrho^2\,\mathrm{d}V = \pi^3 G\mu_\mathrm{c}^2 a^5\left[\left(\lambda + \frac{3}{4}\right)\sigma^{-1} + o(\sigma^{-1})\right]$$

and the integral over the pressure

$$P = \int p\,\mathrm{d}V = \pi^3 G\mu_\mathrm{c}^2 a^5\left(\sigma^{-1} + o(1)\right) \qquad (86)$$

to first order. We see that the virial theorem (49) is fulfilled at the leading order.

For further results see Tables B1–B4.

4.3 Discussion for Homogeneous Rings

With this approximation method, we are able to calculate e.g. the shape, angular velocity and pressure of the ring up to arbitrary order in σ. We have done so up to the 20th order.

An important question is how good this method is. In Tables 1, 2 and 3 one can see how the dimensionless quantities

$$\frac{\hat{M}}{M} = \frac{1}{\mu_\mathrm{c}\varrho_\mathrm{o}^3}, \qquad \frac{\hat{\Omega}^2}{\Omega^2} = \frac{1}{G\mu_\mathrm{c}}, \qquad \frac{\hat{J}}{J} = \frac{1}{G^{1/2}\mu_\mathrm{c}^{3/2}\varrho_\mathrm{o}^5},$$
$$\frac{\hat{P}}{P} = \frac{\hat{T}}{T} = \frac{\hat{W}}{W} = \frac{1}{G\mu_\mathrm{c}^2\varrho_\mathrm{o}^5} \qquad (87)$$

improve in accuracy with increasing order for different radius ratios. Especially for thin rings, we get very accurate results. In fact, for rings with radius ratios $\varrho_\mathrm{i}/\varrho_\mathrm{o} \approx 0.85$ we achieve a precision which is comparable with that given by the numerical method described in Ansorg, Kleinwächter & Meinel (2003a). For larger radius ratios, the accuracy is thus better. As a co-product, our work provides an independent test of the accuracy of the numerical method (better than 10^{-13} cf. Table 1).

The shape of the ring in meridional cross-section for various radius ratios can be found in Fig. 4. The curves to order $q = 20$ can barely be distinguished from the numerical ones for $\varrho_\mathrm{i}/\varrho_\mathrm{o} \gtrsim 0.3$. As one approaches the transition to spheroidal topologies ($\varrho_\mathrm{i}/\varrho_\mathrm{o} \to 0$), the true curve becomes pointy at the inner edge and is no longer well represented by our Fourier series. Nevertheless, the shape of the ring is quite well approximated even for $\varrho_\mathrm{i}/\varrho_\mathrm{o} = 0.1$, as seen in Fig. 5. The surface function $r_\mathrm{s}(\chi)$, which is a constant to leading order, clearly approaches the numerical one with increasing q. The pressure in the equatorial plane can also be seen to approach the numerically determined one for $\varrho_\mathrm{i}/\varrho_\mathrm{o} = 0.3$ in Fig. 6. It is interesting to note that the centre of mass does not coincide with the point of maximum pressure. In Fig. 7 one can get an impression of the accuracy of the approximation over the whole range of radius ratios and for various values of q. Despite the claims found in Wong (1974) that Dyson's perturbative method diverges for $\sigma > 1/3$ (see also the comments in Dyson 1892; Bardeen 1971), these results indicate the opposite.

5 POLYTROPIC RINGS

5.1 Polytropes with Arbitrary Index n

The polytropic equation of state is

$$p = K\mu^{1+1/n}. \qquad (88)$$

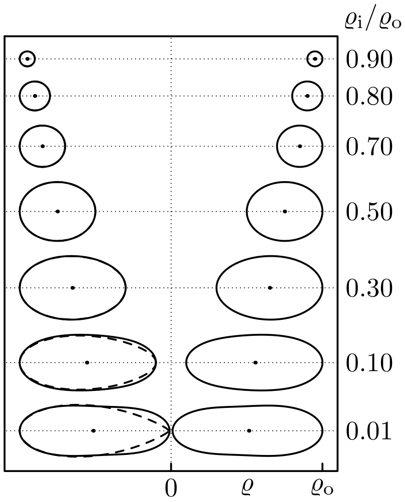

Figure 4. Meridional cross-sections of homogeneous rings to the order $q = 20$ for different radius ratios $\varrho_\mathrm{i}/\varrho_\mathrm{o}$. The ϱ- and z-axis are scaled identically in such a manner that ϱ_o has the same value for all the rings. The dot in each ring marks the centre of mass of the cross-section ($\varrho = b, z = 0$ i.e. $r = 0$) and the dashed line shows the numerical result and is indistinguishable from the $q = 20$ curve for $\varrho_\mathrm{i}/\varrho_\mathrm{o} \gtrsim 0.3$.

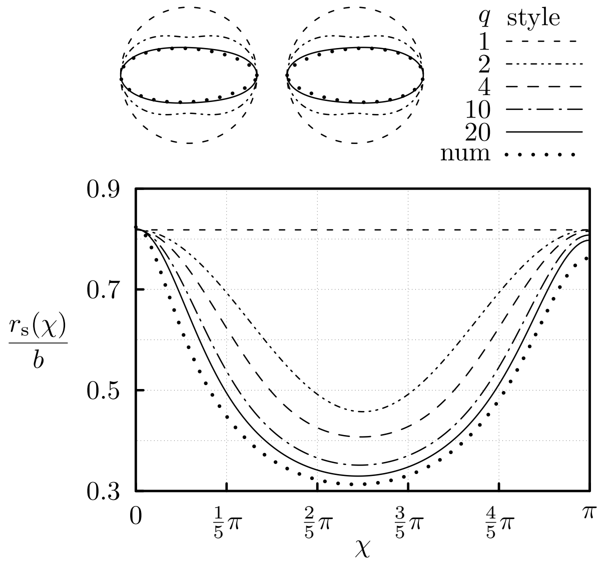

Figure 5. The meridional cross-section and the (dimensionless) surface function $r_\mathrm{s}(\chi)/b$ of the homogeneous ring with radius ratio $\varrho_\mathrm{i}/\varrho_\mathrm{o} = 0.1$ for different orders q compared to the numerical result. The surfaces are scaled such that ϱ_o (and therefore also ϱ_i) has the same value to all orders.

For large/small polytropic indices n, the equation is referred to as 'soft'/'stiff' and it includes homogeneous matter as the limit $\lim_{n\to 0} K^n = 1/\mu = 1/\mu_\mathrm{c}$. From now on, we shall use the terms 'homogeneous matter' and '$n = 0$' interchangeably. For polytropes, (22) becomes

$$4\pi G\mu + K(n+1)\nabla^2\left(\mu^{1/n}\right) - 2\Omega^2 = 0. \qquad (89)$$

Instead of our coordinate y, we are now going to make use of a new dimensionless radial coordinate, applicable to poly-

Table 1. For a given radius ratio $\varrho_\mathrm{i}/\varrho_\mathrm{o} = 0.9$, physical quantities to different orders in q and numerically determined values are compared to the values for $q = 20$: $\hat{M}_{20} = 4.6299179884304816293 \times 10^{-2}$, $\hat{\Omega}^2_{20} = 3.2474683264953211610 \times 10^{-2}$, $\hat{J}_{20} = 7.5456215256289320669 \times 10^{-3}$, $\hat{P}_{20} = 1.7862946528142761708 \times 10^{-4}$, $\hat{T}_{20} = 6.7988816964653749490 \times 10^{-4}$, $\hat{W}_{20} = -1.8956647351373578410 \times 10^{-3}$.

q	σ	$\hat{M}_q/\hat{M}_{20} - 1$	$\hat{\Omega}^2_q/\hat{\Omega}^2_{20} - 1$	$\hat{J}_q/\hat{J}_{20} - 1$	$\hat{P}_q/\hat{P}_{20} - 1$	$\hat{T}_q/\hat{T}_{20} - 1$	$\hat{W}_q/\hat{W}_{20} - 1$
1	0.053	1×10^{-2}	1×10^{-2}	2×10^{-2}	3×10^{-2}	2×10^{-2}	2×10^{-2}
2	0.052	2×10^{-4}	6×10^{-4}	4×10^{-4}	6×10^{-3}	-1×10^{-3}	6×10^{-4}
3	0.052	2×10^{-4}	1×10^{-4}	2×10^{-4}	4×10^{-4}	3×10^{-4}	3×10^{-4}
4	0.052	3×10^{-6}	-1×10^{-5}	-3×10^{-6}	5×10^{-5}	-5×10^{-5}	-2×10^{-5}
10	0.052	6×10^{-11}	-9×10^{-11}	4×10^{-12}	5×10^{-10}	-6×10^{-10}	-3×10^{-10}
19	0.052	4×10^{-17}	4×10^{-17}	6×10^{-17}	1×10^{-16}	9×10^{-17}	9×10^{-17}
num	—	-4×10^{-14}	1×10^{-16}	-4×10^{-14}	-7×10^{-14}	-4×10^{-14}	-3×10^{-14}

Table 2. For a given radius ratio $\varrho_\mathrm{i}/\varrho_\mathrm{o} = 0.5$, physical quantities to different orders in q are compared to the numerically determined values $\hat{M}_\mathrm{num} = 0.7201292$, $\hat{\Omega}^2_\mathrm{num} = 0.5467604$, $\hat{J}_\mathrm{num} = 0.3247949$, $\hat{P}_\mathrm{num} = 0.04874713$, $\hat{T}_\mathrm{num} = 0.1200820$, $\hat{W}_\mathrm{num} = -0.3864053$.

q	σ	$\hat{M}_q/\hat{M}_\mathrm{num} - 1$	$\hat{\Omega}^2_q/\hat{\Omega}^2_\mathrm{num} - 1$	$\hat{J}_q/\hat{J}_\mathrm{num} - 1$	$\hat{P}_q/\hat{P}_\mathrm{num} - 1$	$\hat{T}_q/\hat{T}_\mathrm{num} - 1$	$\hat{W}_q/\hat{W}_\mathrm{num} - 1$
1	0.33	2.8×10^{-1}	2.3×10^{-1}	4.2×10^{-1}	8.6×10^{-1}	4.6×10^{-1}	6.1×10^{-1}
2	0.30	5.1×10^{-2}	5.9×10^{-2}	6.5×10^{-2}	2.5×10^{-1}	2.6×10^{-2}	1.1×10^{-1}
3	0.30	5.1×10^{-2}	4.2×10^{-2}	5.8×10^{-2}	1.3×10^{-1}	8.1×10^{-2}	1.0×10^{-1}
4	0.30	1.7×10^{-2}	1.3×10^{-2}	1.9×10^{-2}	5.4×10^{-2}	8.4×10^{-3}	2.6×10^{-2}
10	0.29	1.2×10^{-3}	1.0×10^{-3}	1.3×10^{-3}	3.2×10^{-3}	1.0×10^{-3}	1.9×10^{-3}
20	0.29	2.6×10^{-5}	2.5×10^{-5}	3.0×10^{-5}	7.2×10^{-5}	2.7×10^{-5}	4.4×10^{-5}

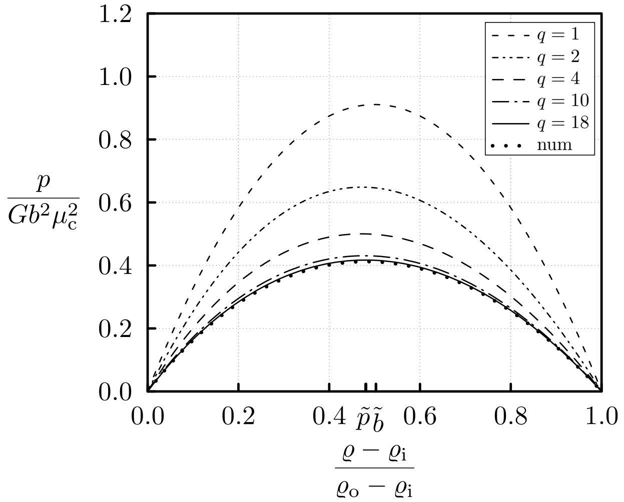

Figure 6. The pressure in the equatorial plane for a homogeneous ring with radius ratio $\varrho_\mathrm{i}/\varrho_\mathrm{o} = 0.3$ for different orders q compared to the numerical result. It is interesting to note that the centre of mass of the cross-section does not coincide with the point of maximum pressure. To the order $q = 18$ we get $\tilde{b} := (b - \varrho_\mathrm{i})/(\varrho_\mathrm{o} - \varrho_\mathrm{i}) = 0.503$ and $\tilde{p} := (\varrho_{\mathrm{p,max}} - \varrho_\mathrm{i})/(\varrho_\mathrm{o} - \varrho_\mathrm{i}) = 0.480$, which differ by less than 1% from the numerical values.

tropes

$$\bar{r} := \frac{G^{\frac{1}{2}} \mu_\mathrm{c}^{\frac{n-1}{2n}}}{K^{\frac{1}{2}}} r. \tag{90}$$

To lowest order in σ, and upon introducing

$$\tilde{\mu} := \mu^{1/n} \tag{91}$$

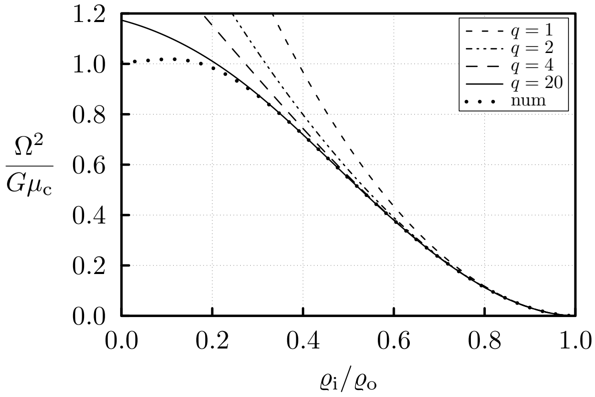

Figure 7. The (dimensionless) squared angular velocity $\Omega^2/G\mu_\mathrm{c}$ as function of the radius ratio $\varrho_\mathrm{i}/\varrho_\mathrm{o}$ for different orders q compared to the numerical result for homogeneous rings.

and the expansion

$$\tilde{\mu} = \mu_\mathrm{c}^{1/n} \left(\sum_{i=0}^{q} \sum_{k=0}^{i} \tilde{\mu}_{ik}(\bar{r}) \cos(k\chi) \sigma^i + o(\sigma^q) \right), \tag{92}$$

equation (89) reads, cf. (35),

$$\left(\frac{\mathrm{d}^2}{\mathrm{d}\bar{r}^2} + \frac{1}{\bar{r}} \frac{\mathrm{d}}{\mathrm{d}\bar{r}} \right) \tilde{\mu}_{00} + \frac{4\pi}{n+1} \tilde{\mu}_{00}^n = 0. \tag{93}$$

This equation is sometimes referred to as one of the *generalized Lane-Emden equations (of the first kind)* and solutions to it have been derived and studied in e.g. Goenner & Havas (2000). No solutions other than for $n = 0$ and $n = 1$ have been found for our particular parameters in closed-form and a discussion using symmetry transformations suggests that they do not exist, (Goenner 2001). In the limiting case $n = 0$, this equation provides an alternative, but less transparent,

Table 3. For a given radius ratio $\varrho_\mathrm{i}/\varrho_\mathrm{o} = 0.2$, physical quantities to different orders in q are compared to the numerically determined values $\hat{M}_\mathrm{num} = 0.9424$, $\hat{\Omega}^2_\mathrm{num} = 0.9844$, $\hat{J}_\mathrm{num} = 0.4545$, $\hat{P}_\mathrm{num} = 0.07865$, $\hat{T}_\mathrm{num} = 0.2255$, $\hat{W}_\mathrm{num} = -0.6869$.

q	σ	$\hat{M}_q/\hat{M}_\mathrm{num} - 1$	$\hat{\Omega}^2_q/\hat{\Omega}^2_\mathrm{num} - 1$	$\hat{J}_q/\hat{J}_\mathrm{num} - 1$	$\hat{P}_q/\hat{P}_\mathrm{num} - 1$	$\hat{T}_q/\hat{T}_\mathrm{num} - 1$	$\hat{W}_q/\hat{W}_\mathrm{num} - 1$
1	0.67	1.0	7.5×10^{-1}	1.6	5.1	1.6	2.8
2	0.54	3.2×10^{-1}	3.5×10^{-1}	3.9×10^{-1}	1.6	3.2×10^{-1}	7.6×10^{-1}
3	0.54	3.2×10^{-1}	2.7×10^{-1}	3.5×10^{-1}	1.1	5.4×10^{-1}	7.2×10^{-1}
4	0.51	1.9×10^{-1}	1.7×10^{-1}	2.1×10^{-1}	6.3×10^{-1}	2.1×10^{-1}	3.6×10^{-1}
10	0.47	6.4×10^{-2}	6.9×10^{-2}	7.1×10^{-2}	1.9×10^{-1}	8.7×10^{-2}	1.2×10^{-1}
20	0.46	2.2×10^{-2}	2.7×10^{-2}	2.3×10^{-2}	6.0×10^{-2}	3.2×10^{-2}	4.2×10^{-2}

method to the one presented above for treating homogeneous matter to lowest order. We concentrate in the next section on the special case $n = 1$.

For other polytropic indices, the iterative method presented here can be applied with the help of numerics. By describing the unknown density terms $\tilde{\mu}_{ik}$ using Chebyshev polynomials and expanding all the quantities involved in terms of λ, equations can be formulated for purely numerical coefficients. The equations of the approximation scheme described in Section 2 must be fulfilled, whereby the ODEs for $\tilde{\mu}_{ik}$ are evaluated at collocation points of the Chebyshev polynomials. In general, the density functions $\tilde{\mu}_{00}$ are not analytic at $\bar{r} = \bar{a}$, meaning that high order polynomials may be necessary to find a good approximation of the function desired. We none the less chose this method, since the equations involve integrals over the density for which one endpoint of integration contains the unknown surface function $r_\mathrm{s}(\chi)$, making their polynomial representation particularly useful.

If one is only interested in determining $\bar{a}$, β_{11} and Ω_2, then it is not necessary to combine such numerical and algebraic techniques and one can choose any numerical method for solving the ODEs. One begins by solving equation (93) numerically for the desired polytropic index n, prescribing the 'initial conditions' $\tilde{\mu}_{00}(0) = 1$ and $\frac{\mathrm{d}}{\mathrm{d}\bar{r}}\tilde{\mu}_{00}\big|_{\bar{r}=0} = 0$. For spherical polytropic fluids, a surface of vanishing pressure is known to exist only for $n < 5$, where the surface for $n = 5$ extends out to infinity. The situation for polytropic rings is quite different – it seems that arbitrarily large polytropic indices are possible! Numerical solutions to (93) indicate that the density function μ_{00} indeed falls to zero for large n. The value of $\bar{r}$ at the first zero of the solution is $\bar{a}$. One then proceeds to solve equation

$$\left(\frac{\mathrm{d}^2}{\mathrm{d}\bar{r}^2} + \frac{1}{\bar{r}}\frac{\mathrm{d}}{\mathrm{d}\bar{r}} - \frac{1}{\bar{r}^2}\right)\tilde{\mu}_{11} + \frac{4\pi n}{n+1}\tilde{\mu}_{00}^{n-1}\tilde{\mu}_{11} = \frac{1}{\bar{a}}\frac{\mathrm{d}\tilde{\mu}_{00}}{\mathrm{d}\bar{r}} \tag{94}$$

for $\tilde{\mu}_{11}$ with the condition $\tilde{\mu}_{11}(0) = 0$ and where $\frac{\mathrm{d}}{\mathrm{d}\bar{r}}\tilde{\mu}_{11}\big|_{\bar{r}=0}$ has to be chosen so as to fulfil the centre of mass condition (3) to first order, which reads (cf. (43))

$$\begin{aligned} 0 &= \int\limits_0^{\bar{a}} \mu_{11}\bar{r}^2\,\mathrm{d}\bar{r} = n\int\limits_0^{\bar{a}} \tilde{\mu}_{00}^{n-1}\tilde{\mu}_{11}\bar{r}^2\,\mathrm{d}\bar{r} \\ \Longrightarrow 0 &= \bar{a}^2\left.\frac{\mathrm{d}\tilde{\mu}_{11}}{\mathrm{d}\bar{r}}\right|_{\bar{r}=\bar{a}} - \bar{a}\tilde{\mu}_{11}(\bar{a}) + \frac{2}{\bar{a}}\int\limits_0^{\bar{a}}\tilde{\mu}_{00}\bar{r}\,\mathrm{d}\bar{r}. \end{aligned} \tag{95}$$

Table 4. The values of expansion coefficients for the surface function $r_\mathrm{s}(\chi)$ and for the squared angular velocity are provided up to first order for different polytropic indices n. The value of $\bar{a}$ for $n = 0$ can be found by solving (93) with $n = 0$ and the conditions $\frac{\mathrm{d}}{\mathrm{d}\bar{r}}\tilde{\mu}_{00}|_{\bar{r}=0} = 0$ and $\tilde{\mu}_{00}(0) = 1$ and then locating the first zero of $\tilde{\mu}_{00}$.

n	$\bar{a}$	β_{11}	Ω_2
0	$1/\sqrt{\pi} \approx 0.5642$	0	$\lambda + 3/4$
0.5	0.7566	-0.03537	$0.6371\lambda + 0.5575$
1	0.9594	-0.07708	$0.4318(\lambda + 1)$
2	1.427	-0.1731	$0.2169\lambda + 0.2711$
5	3.750	-0.5118	$0.03614\lambda + 0.07228$
10	15.18	-1.126	$(2.401\lambda + 7.804) \times 10^{-3}$
20	207.6	-2.375	$(1.362\lambda + 7.829) \times 10^{-5}$
30	2.661×10^3	-3.625	$(8.487\lambda + 70.02) \times 10^{-8}$
40	3.337×10^4	-4.875	$(5.468\lambda + 58.78) \times 10^{-10}$
50	4.142×10^5	-6.125	$(3.577\lambda + 47.40) \times 10^{-12}$

The constant β_{11} can then be found using equation (39), which now reads

$$\beta_{11} = -\frac{\tilde{\mu}_{11}(\bar{a})}{\bar{a}}\left(\frac{\mathrm{d}\tilde{\mu}_{00}}{\mathrm{d}\bar{r}}\right)^{-1}\Bigg|_{\bar{r}=\bar{a}}, \tag{96}$$

and Ω_2 is taken from (53). The behaviour of these coefficients as they depend on the polytropic index n can be found in Table 4. The table suggests that $\bar{a} \to \infty$ and $\Omega_2 \to 0$ exponentially in n for $n \to \infty$, which is indeed known to hold (Ostriker 1964a,b). The behaviour of the specific kinetic energy of a particle in the ring, proportional to $\bar{a}^2\Omega_2$ to leading order, will be discussed in Section 6 together with the behaviour of β_{11} for large n.

We provide a comparison of precise numerical values for various (dimensionless) physical quantities with their first and third order equivalents in Table 5. The dimensionless quantities, valid for any polytropic index $n > 0$ are

$$\begin{aligned} &\frac{\bar{M}}{M} = \frac{G^{\frac{3}{2}}\mu_\mathrm{c}^{\frac{n-3}{2n}}}{K^{\frac{3}{2}}}, \quad \frac{\bar{J}}{J} = \frac{G^2\mu_\mathrm{c}^{\frac{2n-5}{2n}}}{K^{\frac{5}{2}}}, \quad \frac{\bar{\Omega}}{\Omega} = \frac{1}{G^{\frac{1}{2}}\mu_\mathrm{c}^{\frac{1}{2}}}, \\ &\frac{\bar{P}}{P} = \frac{\bar{T}}{T} = \frac{\bar{W}}{W} = \frac{G^{\frac{3}{2}}\mu_\mathrm{c}^{\frac{n-5}{2n}}}{K^{\frac{5}{2}}}, \quad \frac{\bar{b}}{b} = \frac{\bar{\varrho}}{\varrho} = \frac{G^{\frac{1}{2}}\mu_\mathrm{c}^{\frac{n-1}{2n}}}{K^{\frac{1}{2}}}. \end{aligned} \tag{97}$$

One can see that the accuracy of the method does not depend strongly on the polytropic index and that relative errors at third order are well below one percent for rings with a radius ratio of 0.9.

Table 5. Physical quantities to the first and third order in σ are compared to the correct, numerically determined values for given polytropic index n and given radius ratio $\varrho_\mathrm{i}/\varrho_\mathrm{o} = 0.9$. The polytropic indices $n = 1.5$ and $n = 3$ correspond to a non-relativistic and ultra-relativistic completely degenerate Fermi gas respectively.

n	q	$\bar{M}$	$\bar{\Omega}^2$	$\bar{J}$	$\bar{P}$	$\bar{T}$	$\bar{W}$
1	1	143.0	1.512×10^{-2}	5.839×10^3	89.24	359.1	−985.8
1	3	144.3	1.499×10^{-2}	5.952×10^3	90.06	364.4	−998.9
1	num	144.3	1.499×10^{-2}	5.953×10^3	90.07	364.5	−999.2
1.5	1	186.9	1.094×10^{-2}	9.836×10^3	124.0	514.3	−1401
1.5	3	188.5	1.084×10^{-2}	1.001×10^4	125.0	521.0	−1417
1.5	num	188.6	1.084×10^{-2}	1.001×10^4	125.0	521.1	−1417
3	1	356.0	4.569×10^{-3}	3.527×10^4	263.5	1192	−3174
3	3	358.7	4.524×10^{-3}	3.581×10^4	265.4	1204	−3205
3	num	358.8	4.523×10^{-3}	3.582×10^4	265.5	1204	−3205
5	1	714.0	1.584×10^{-3}	1.439×10^5	570.2	2864	−7438
5	3	719.9	1.563×10^{-3}	1.464×10^5	574.8	2893	−7511
5	num	720.0	1.563×10^{-3}	1.464×10^5	574.9	2894	−7513

5.2 Analytic Solution for Polytropes with $n = 1$

5.2.1 The Zeroth Order: σ^0

We rewrite (93) for $n = 1$, remembering that now $\tilde{\mu} = \mu$,

$$\left(\frac{\mathrm{d}^2}{\mathrm{d}\bar{r}^2} + \frac{1}{\bar{r}}\frac{\mathrm{d}}{\mathrm{d}\bar{r}}\right)\mu_{00} + 2\pi\mu_{00} = 0 \tag{98}$$

and can immediately write down the general solution

$$\mu_{00} = C_1 J_0(\sqrt{2\pi}\bar{r}) + C_2 Y_0(\sqrt{2\pi}\bar{r}), \tag{99}$$

where J_n is a Bessel function (of the first kind) and Y_n a Neumann function (also called a Bessel function of the second kind), see e.g. Prudnikov, Brychkov & Marichev (1990). The condition $\mu(r = 0, \chi) = \mu_\mathrm{c}$ tells us that $C_1 = 1$ and $C_2 = 0$. The first positive zero of J_0 determines value for a from (12). We refer to the kth positive zero of the nth Bessel function as j_{nk} and can then write

$$\bar{a} := a\bar{r}/r = j_{01}/\sqrt{2\pi} = 0.959\ldots \tag{100}$$

The value for $a = \bar{a}\sqrt{K/G}$ is independent of the choice of μ_c, which is not the case for other polytropic indices. This is due to an interesting invariance for $n = 1$: if $U(\boldsymbol{x})$, $\mu(\boldsymbol{x}) = K\sqrt{p(\boldsymbol{x})}$ and $\boldsymbol{v}(\boldsymbol{x})$ are solutions to the Poisson and Euler equations, then so are $\alpha U(\boldsymbol{x})$, $\alpha\mu(\boldsymbol{x}) = K\sqrt{\alpha^2 p(\boldsymbol{x})}$ and $\sqrt{\alpha}\boldsymbol{v}(\boldsymbol{x})$, where α is an arbitrary scaling factor.

5.2.2 The First Order: σ^1

The unknown quantities we have to solve for are $\mu_{10}(\bar{r})$, $\mu_{11}(\bar{r})$, β_{10}, β_{11} and Ω_2. From (22), one finds the differential equations

$$\left(\frac{\mathrm{d}^2}{\mathrm{d}\bar{r}^2} + \frac{1}{\bar{r}}\frac{\mathrm{d}}{\mathrm{d}\bar{r}}\right)\mu_{10} + 2\pi\mu_{10} = 0 \tag{101}$$

and

$$\left(\frac{\mathrm{d}^2}{\mathrm{d}\bar{r}^2} + \frac{1}{\bar{r}}\frac{\mathrm{d}}{\mathrm{d}\bar{r}}\right)\mu_{11} + \left(2\pi - \frac{1}{\bar{r}^2}\right)\mu_{11} = \frac{1}{\bar{a}}\frac{\mathrm{d}\mu_{00}}{\mathrm{d}\bar{r}}. \tag{102}$$

Considering only solutions that vanish at the point $\bar{r} = 0$, so as to maintain our choice $\mu(0) = \mu_\mathrm{c}$, we find

$$\mu_{10} = 0 \tag{103}$$

and

$$\mu_{11} = C_3 J_1 + \frac{1}{2j_{01}}\left(\sqrt{2\pi}\bar{r}J_0 - J_1\right), \tag{104}$$

where the argument of the Bessel functions is always $\sqrt{2\pi}\bar{r}$ unless otherwise specified. The requirement that the density vanish at the surface of the rings determines

$$\beta_{10} = 0 \tag{105}$$

and relates the constant C_3 to the surface function

$$C_3 = \frac{1 + 2j_{01}^2\beta_{11}}{2j_{01}}. \tag{106}$$

The constant β_{11} is determined by stipulating that the centre of mass coincide with the point ($\varrho = b, z = 0$) as in (3)

$$\beta_{11} = \frac{4 - j_{01}^2}{4j_{01}^2}. \tag{107}$$

Recalling the definition $\lambda := \ln\frac{8}{\sigma} - 2$, one finally obtains

$$\Omega_2 = \frac{2J_1(j_{01})(\lambda + 1)}{j_{01}} \tag{108}$$

from (11).

5.2.3 The Second Order: σ^2

To second order, the unknown quantities that have to be solved for are $\mu_{20}(\bar{r})$, $\mu_{21}(\bar{r})$, $\mu_{22}(\bar{r})$, β_{20}, β_{21}, β_{22} and Ω_3.

The ODEs describing the mass density now read

$$\begin{aligned}\left(\frac{\mathrm{d}^2}{\mathrm{d}\bar{r}^2} + \frac{1}{\bar{r}}\frac{\mathrm{d}}{\mathrm{d}\bar{r}}\right)\mu_{20} + 2\pi\mu_{20} &= \pi\Omega_2 \\ &+ \frac{1}{2\bar{a}}\left(\frac{\mathrm{d}\mu_{11}}{\mathrm{d}\bar{r}} - \frac{\mu_{11}}{\bar{r}}\right) + \frac{\bar{r}}{2\bar{a}^2}\frac{\mathrm{d}\mu_{00}}{\mathrm{d}\bar{r}},\end{aligned} \tag{109}$$

$$\left(\frac{\mathrm{d}^2}{\mathrm{d}\bar{r}^2} + \frac{1}{\bar{r}}\frac{\mathrm{d}}{\mathrm{d}\bar{r}}\right)\mu_{21} + \left(2\pi - \frac{1}{\bar{r}^2}\right)\mu_{21} - \frac{1}{\bar{a}}\frac{\mathrm{d}\mu_{10}}{\mathrm{d}\bar{r}} = 0 \tag{110}$$

and

$$\begin{aligned}\left(\frac{\mathrm{d}^2}{\mathrm{d}\bar{r}^2} + \frac{1}{\bar{r}}\frac{\mathrm{d}}{\mathrm{d}\bar{r}}\right)\mu_{22} + \left(2\pi - \frac{4}{\bar{r}^2}\right)\mu_{22} &= \\ \frac{1}{2\bar{a}}\left(\frac{\mathrm{d}\mu_{11}}{\mathrm{d}\bar{r}} - \frac{\mu_{11}}{\bar{r}}\right) + \frac{\bar{r}}{2\bar{a}^2}\frac{\mathrm{d}\mu_{00}}{\mathrm{d}\bar{r}}.&\end{aligned} \tag{111}$$

The solutions vanishing at $\bar{r} = 0$ are

$$\mu_{20} = \frac{\Omega_2}{2}\left(1 - J_0\right) + \frac{1}{8}\left[\frac{3\pi\bar{r}^2}{j_{01}^2} J_0 + \sqrt{2\pi}\bar{r}\left(\frac{1}{j_{01}^2} - \frac{1}{2}\right) J_1\right], \tag{112}$$

$$\mu_{21} = C_4 J_1 \tag{113}$$

and

$$\begin{aligned}\mu_{22} = C_5 J_2 + \frac{1}{4}\bigg[&\left(\frac{5}{j_{01}^2} + \frac{3\pi\bar{r}^2}{2j_{01}^2} - \frac{1}{2}\right) J_2 \\ &+ \frac{\sqrt{\pi}\bar{r}}{\sqrt{2}}\left(\frac{5}{j_{01}^2} - \frac{1}{2}\right) J_1\bigg].\end{aligned} \tag{114}$$

The constants C_4 and C_5 can be related to the surface function by requiring that $\mu(r_\mathrm{s}) = 0$ hold independently for the coefficients in front of $\cos\chi$ and $\cos 2\chi$. The result is

$$C_4 = j_{01}\beta_{21} \tag{115}$$

and

$$C_5 = \frac{1}{2}\left(-j_{01}^2\beta_{22} - \frac{j_{01}^2}{64} + \frac{3}{8} - \frac{11}{4j_{01}^2}\right). \tag{116}$$

Requiring the same of the coefficient in front of $\cos 0\chi$ gives

$$\beta_{20} = -\frac{4}{j_{01}^4} + \frac{\lambda + 1}{j_{01}^2} - \frac{1}{64}. \tag{117}$$

Evaluating (3) tells us that

$$\beta_{21} = 0 \Longrightarrow \mu_{21} = 0. \tag{118}$$

The values for the remaining constants follow from (11):

$$\Omega_3 = 0 \tag{119}$$

and

$$\beta_{22} = \frac{1}{4j_{01}^4} + \frac{5(\lambda + 3)}{2j_{01}^2} + \frac{1}{64}. \tag{120}$$

5.2.4 *The Third Order: σ^3*

The third order is the final one to be presented here, but the iterative scheme can be applied up to arbitrary order assuming that one is able to solve the differential equations for the mass density and perform the necessary integrals. The ODEs that result for this order are

$$\left(\frac{\mathrm{d}^2}{\mathrm{d}\bar{r}^2} + \frac{1}{\bar{r}}\frac{\mathrm{d}}{\mathrm{d}\bar{r}}\right)\mu_{30} + 2\pi\mu_{30} = 0, \tag{121}$$

$$\begin{aligned}\left(\frac{\mathrm{d}^2}{\mathrm{d}\bar{r}^2} + \frac{1}{\bar{r}}\frac{\mathrm{d}}{\mathrm{d}\bar{r}}\right)\mu_{31} + \left(2\pi - \frac{1}{\bar{r}^2}\right)\mu_{31} = \frac{3\bar{r}^2}{4\bar{a}^3}\frac{\mathrm{d}\mu_{00}}{\mathrm{d}\bar{r}} \\ + \frac{3}{4\bar{a}^2}\left(\bar{r}\frac{\mathrm{d}}{\mathrm{d}\bar{r}} + 1\right)\mu_{11} + \frac{1}{\bar{a}}\left[\frac{\mathrm{d}\mu_{20}}{\mathrm{d}\bar{r}} + \left(\frac{1}{2}\frac{\mathrm{d}}{\mathrm{d}\bar{r}} + \frac{1}{\bar{r}}\right)\mu_{22}\right],\end{aligned} \tag{122}$$

$$\left(\frac{\mathrm{d}^2}{\mathrm{d}\bar{r}^2} + \frac{1}{\bar{r}}\frac{\mathrm{d}}{\mathrm{d}\bar{r}}\right)\mu_{32} + 2\left(\pi - \frac{2}{\bar{r}^2}\right)\mu_{32} = 0 \tag{123}$$

and

$$\begin{aligned}\left(\frac{\mathrm{d}^2}{\mathrm{d}\bar{r}^2} + \frac{1}{\bar{r}}\frac{\mathrm{d}}{\mathrm{d}\bar{r}}\right)\mu_{33} + \left(2\pi - \frac{9}{\bar{r}^2}\right)\mu_{33} = \frac{\bar{r}^2}{4\bar{a}^3}\frac{\mathrm{d}\mu_{00}}{\mathrm{d}\bar{r}} \\ + \frac{1}{4\bar{a}^2}\left(\bar{r}\frac{\mathrm{d}}{\mathrm{d}\bar{r}} - 1\right)\mu_{11} + \frac{1}{\bar{a}}\left(\frac{1}{2}\frac{\mathrm{d}}{\mathrm{d}\bar{r}} - \frac{1}{\bar{r}}\right)\mu_{22}.\end{aligned} \tag{124}$$

The solutions to these equations obeying the requirement $\mu_{qk}(0) = 0$ are

$$\mu_{30} = 0, \tag{125}$$

$$\begin{aligned}\mu_{31} = &\left(C_6 - \frac{(\lambda + 1)\, J_1(j_{01})}{2j_{01}^2} - \frac{9}{64}\frac{\pi\left(j_{01}^2 - 8\right)\bar{r}^2}{j_{01}^3}\right. \\ &\left.- \frac{j_{01}^4 + 16j_{01}^2(5\lambda + 4) - 16}{256j_{01}^3}\right) J_1 \\ &+ \left(\frac{\sqrt{\pi}\,(\lambda + 1)\, J_1(j_{01})\,\bar{r}}{\sqrt{2}j_{01}^2} - \frac{15}{32}\frac{\sqrt{2}\pi^{3/2}\bar{r}^3}{j_{01}^3}\right. \\ &\left.+ \frac{\sqrt{2\pi}\left(j_{01}^4 + 16j_{01}^2(5\lambda + 4) - 16\right)\bar{r}}{256j_{01}^3}\right) J_2,\end{aligned} \tag{126}$$

$$\mu_{32} = C_7 J_2 \tag{127}$$

and

$$\begin{aligned}\mu_{33} = &\frac{\pi\bar{r}^2\left(16j_{01}^2(5\lambda + 2) - 40\pi\bar{r}^2 + 272 + j_{01}^4\right)}{512j_{01}^3} J_1 \\ &+ \left(-\frac{5\pi^2\bar{r}^4}{64j_{01}^3} + \frac{\pi\left(j_{01}^4 + 8j_{01}^2(10\lambda + 7) + 16\right)\bar{r}^2}{512j_{01}^3}\right. \\ &\left.- \frac{3\left(j_{01}^4 + 16j_{01}^2(5\lambda + 3) + 208\right)}{256j_{01}^3} + C_8\right) J_3.\end{aligned} \tag{128}$$

The constants β_{30}, C_6, C_7 and C_8 are determined by requiring that $\mu(r = r_\mathrm{s}) = 0$ hold independently for the coefficients in front of the $\cos 0\chi$, $\cos\chi$, $\cos 2\chi$ and $\cos 3\chi$ terms. The result is

$$\begin{aligned}\beta_{30} &= 0, \\ C_6 &= \left(\frac{\lambda + 1}{4} - \frac{3\,(\lambda + 1)}{2j_{01}^2}\right) J_1(j_{01}) - \frac{j_{01}^3}{512} \\ &\quad + j_{01}\left(\frac{5}{32}\lambda + \beta_{31} + \frac{39}{256}\right) \\ &\quad - \frac{14\lambda + 9}{32j_{01}} + \frac{40\lambda + 37}{16j_{01}^3},\end{aligned} \tag{129}$$

$$C_7 = 0 \tag{130}$$

and

$$\begin{aligned}C_8 = \frac{1}{j_{01}^2 - 8}\bigg[&-\frac{j_{01}^5}{1536} - \left(\frac{5}{32}\lambda + \beta_{33} + \frac{77}{768}\right) j_{01}^3 \\ &+ \left(\frac{35}{16}\lambda + \frac{11}{8}\right) j_{01} - \frac{1}{j_{01}}\left(10\lambda + \frac{181}{48}\right) - \frac{119}{6j_{01}^3}\bigg].\end{aligned} \tag{131}$$

Equation (3) yields

$$\beta_{31} = \frac{9}{32}\lambda + \frac{31}{128} - \frac{1}{j_{01}^2}\left(\frac{13}{8}\lambda + \frac{5}{16}\right) - \frac{1}{j_{01}^4}\left(\frac{5}{2}\lambda + 9\right) \tag{132}$$

and (11) gives

$$\beta_{32} = 0, \tag{133}$$

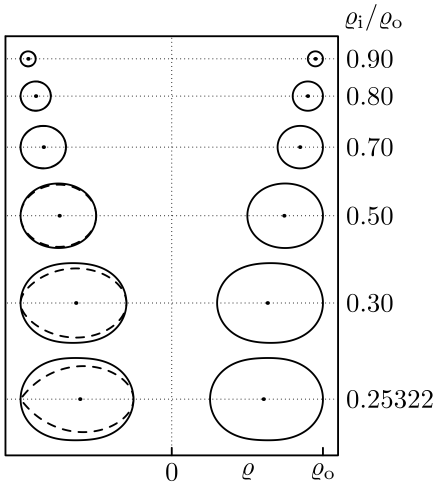

Figure 8. Meridional cross-sections of polytropic rings ($n = 1$) with varying radius ratio are shown to third order (solid lines) in comparison to numerical results (dashed lines) for the same radius ratio. At the value $\varrho_{\rm i}/\varrho_{\rm o} = 0.25322\ldots$, the rings reach a mass-shedding limit, as is evident from the numerical cross-section.

$$\begin{aligned}\Omega_4 = {} & -2\frac{(\lambda+1)^2}{j_{01}^2}J_1(j_{01})^2 + \Bigg[\frac{1}{32}(\lambda+1)\,j_{01} \\ & + \frac{1}{j_{01}}\left(\lambda^2+\frac{3}{8}\lambda-\frac{1}{2}\right) \\ & + \frac{1}{j_{01}^3}\left(\frac{11}{2}\lambda+\frac{17}{4}\right)\Bigg]J_1(j_{01})\end{aligned} \tag{134}$$

and

$$\beta_{33} = \frac{5}{64} - \frac{1}{8j_{01}^2}(5\lambda+9) + \frac{1}{j_{01}^4}\left(\frac{5}{2}\lambda+2\right). \tag{135}$$

5.2.5 *Physical Parameters to the Third Order*

The shape of the rings to third order that results from equation (12) is compared to numerical results of the corresponding radius ratio in Fig. 8. For thin rings, the numerical and third order curves are indistinguishable. As the radius ratio is decreased, the numerical results show that the outer edge becomes pointier, right up to the mass-shedding limit for the value $\varrho_{\rm i}/\varrho_{\rm o} = 0.25322\ldots$. For such a ring, a fluid particle rotating at the outer rim in the equatorial plane has a rotational frequency equal to the Kepler frequency, meaning that it is kept in balance by the gravitational and centrifugal forces alone – the force arising from the pressure gradient vanishes. The shape of the ring with the cusp that forms for mass-shedding configurations is not well represented by a small number of terms in our Fourier series.

Using the results of the last subsection, we write down expressions for various physical parameters and can use them to verify that the virial identity (49) is satisfied to each order in σ. Up to and including third order one finds

$$\begin{aligned}\bar M = {} & \frac{\sqrt{2\pi}j_{01}^2J_1(j_{01})}{\sigma} \\ & + \Bigg[\frac{\sqrt{2\pi}}{64}\left(j_{01}^4+28j_{01}^2+32j_{01}^2\lambda-16\right)J_1(j_{01}) \\ & - \sqrt{2\pi}j_{01}\,(\lambda+1)\,J_1(j_{01})^2\Bigg]\sigma,\end{aligned} \tag{136}$$

$$\begin{aligned}\bar J = {} & \sqrt{\frac{J_1(j_{01})\,(\lambda+1)}{j_{01}}}J_1(j_{01})\,j_{01}^2\Bigg\{\frac{j_{01}^2}{\sigma^2} \\ & - \frac{3}{2}(\lambda+1)\,j_{01}J_1(j_{01}) \\ & + \frac{1}{128\,(\lambda+1)}\big[3j_{01}^4(\lambda+1) \\ & + j_{01}^2(96\lambda^2+324\lambda+232)-624\lambda-664\big]\Bigg\},\end{aligned} \tag{137}$$

$$\begin{aligned}\bar P = {} & \frac{\sqrt{2\pi}}{2}j_{01}J_1(j_{01})^2\Bigg\{\frac{j_{01}^2}{\sigma} \\ & + \frac{1}{320}\Big[-640j_{01}\,(\lambda+1)\,J_1(j_{01}) \\ & + 10\left(j_{01}^4-8j_{01}^2+128\lambda+136\right)\Big]\sigma\Bigg\},\end{aligned} \tag{138}$$

$$\begin{aligned}\bar T = {} & \frac{\sqrt{2\pi}}{2}J_1(j_{01})^2\,j_{01}\Bigg\{\frac{1}{\sigma}(\lambda+1)\,j_{01}^2 \\ & + \Big[-2\,(\lambda+1)^2J_1(j_{01})\,j_{01} + \frac{1}{32}\Big(j_{01}^4(\lambda+1) \\ & + 2j_{01}^2(8\lambda+9)(2\lambda+3)-112\lambda-132\Big)\Big]\sigma\Bigg\}\end{aligned} \tag{139}$$

and

$$\begin{aligned}\bar W = {} & \sqrt{2\pi}j_{01}J_1(j_{01})^2\Bigg\{-\frac{j_{01}^2}{2\sigma}(2\lambda+5) \\ & + \Bigg[j_{01}\,(2\lambda+5)\,(\lambda+1)\,J_1(j_{01}) \\ & - \frac{1}{64}\Big(j_{01}^4(2\lambda+5)+4j_{01}^2(16\lambda^2+42\lambda+21) \\ & \quad + 160\lambda+144\Big)\Bigg]\sigma\Bigg\}.\end{aligned} \tag{140}$$

In the derivation of the above expressions for $\bar P$ and $\bar W$, we have made use of the identity

$$20\,{}_2F_3\left(\frac{3}{2},\frac{3}{2};2,2,\frac{5}{2};-j_{01}^2\right) = 3j_{01}^2\,{}_2F_3\left(\frac{5}{2},\frac{5}{2};3,3,\frac{7}{2};-j_{01}^2\right) \tag{141}$$

for the Gauss hypergeometric function

$$\begin{aligned}& {}_pF_q(a_1,a_2,\ldots,a_p;b_1,b_2,\ldots,b_q;z) \\ & \quad := \sum_{k=0}^{\infty}\frac{(a_1)_k\cdot(a_2)_k\cdots(a_p)_k}{(b_1)_k\cdot(b_2)_k\cdots(b_q)_k}\frac{z^k}{k!}\end{aligned} \tag{142}$$

with the Pochhammer bracket

$$(a)_k := a(a+1)\cdots(a+k-1), \qquad (a)_0 := 1.$$

A proof of (141) can be found in Appendix A.

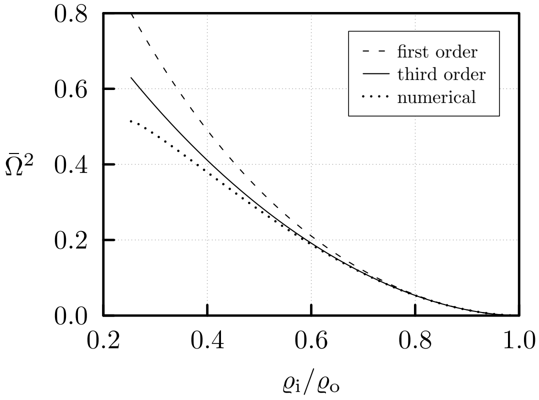

Figure 9. The square of the dimensionless angular velocity is plotted versus the radius ratio for rings with polytropic index $n = 1$.

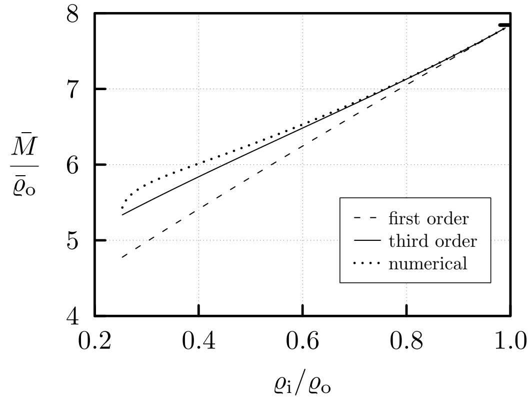

Figure 10. The dimensionless mass divided by the outer radius is plotted versus the radius ratio for rings with polytropic index $n = 1$. This quantity tends to the value $\bar{M}/\bar{\varrho}_\mathrm{o} = 2\pi j_{01} J_1(j_{01}) = 7.84\ldots$ in the thin ring limit, which is marked by a tick.

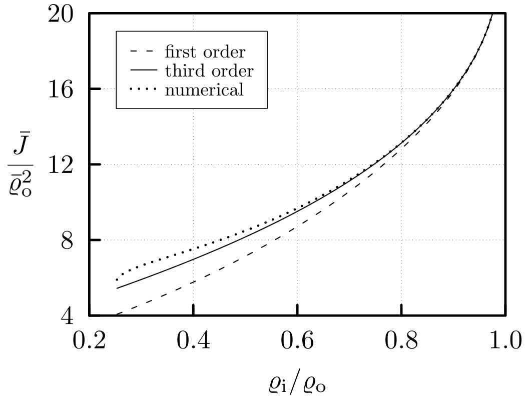

Figure 11. The dimensionless angular momentum divided by the square of the outer radius is plotted versus the radius ratio for rings with polytropic index $n = 1$. This quantity as a function of radius ratio tends logarithmically to infinity.

In order to gauge the accuracy of the expressions listed above, some of them are plotted to first and third order in comparison to numerical values in Figs 9–11. The accuracy of the numerical values is high enough so as to render the corresponding curve indistinguishable from the 'correct' one and is plotted in its entirety, i.e. from the thin ring limit right up to the mass-shedding limit. The curves to first and third order were drawn by taking the expression for $\bar{\varrho}_\mathrm{i}$, $\bar{\varrho}_\mathrm{o}$, $\bar{\Omega}^2$, $\bar{M}$ and $\bar{J}$ to first and third order respectively, inserting a numerical value for σ and then taking the appropriate combination of these numbers. One finds in all three plots that the third order brings a marked improvement as compared to the first one, but that the behaviour near the mass-shedding limit is not particularly well represented.

6 A LIMIT OF INFINITE POLYTROPIC INDEX

As n tends to infinity, the polytropic equation (88) shows us that pressure and density are proportional

$$p = K\mu, \tag{143}$$

a case sometimes referred to as 'isothermal' because such an equation holds for an ideal gas at constant temperature. Inserting this into equation (22) at leading order and again using the dimensionless coordinate $\bar{r}$ yields

$$4\pi\bar{r}\mu_{00} + \frac{\mathrm{d}}{\mathrm{d}\bar{r}}\left(\bar{r}\frac{\mathrm{d}}{\mathrm{d}\bar{r}}\ln\mu_{00}\right) = 0. \tag{144}$$

The solution to this equation with our normalization $\mu_{00}(\bar{r} = 0) = 1$ reads

$$\mu_{00} = \left(\frac{\pi}{2}\bar{r}^2 + 1\right)^{-2}. \tag{145}$$

The density and pressure fall to zero as $\bar{r} \to \infty \Leftrightarrow r \to \infty$. Integrating over the density to calculate the normalized mass, one finds to leading order

$$\bar{M} = 4\pi^2\bar{b}\int_0^\infty \mu_{00}\bar{r}\,\mathrm{d}\bar{r} = 4\pi\bar{b}, \tag{146}$$

which can also be read off from equation (42) directly, by making use of $\bar{M} = \bar{P}$, which is self-evident upon taking (143) into account. In Fig. 12, the behaviour of $\bar{M}/4\pi\bar{b}$ can be followed from the homogeneous case, $n = 0$, right up to the isothermal limit $n \to \infty$.

Making use of (145), we find that

$$\lim_{n\to\infty} g = 0, \tag{147}$$

where g was defined in (45). It thus follows from (52) that

$$\lim_{n\to\infty}\left(\beta_{11} + \frac{n}{8}\right) = \frac{1}{8} \tag{148}$$

as already suggested by the results of Table 4. We can then see that the specific kinetic energy $\bar{a}^2\Omega_2$ tends to infinity such that for fixed λ

$$\lim_{n\to\infty}\frac{2\pi\bar{a}^2\Omega_2}{n + 4\lambda} = 1. \tag{149}$$

From the fact that $|\beta_{11}|$ tends to infinity, we can conclude that the range of σ values for which the first order provides a good approximation shrinks to the point $\sigma = 0$. In general, for a given equation of state, there exist ring solutions over an interval of radius ratios ranging from 1 in the thin ring limit down to a minimal value at the mass-shedding limit. The numerical values presented in Table 6

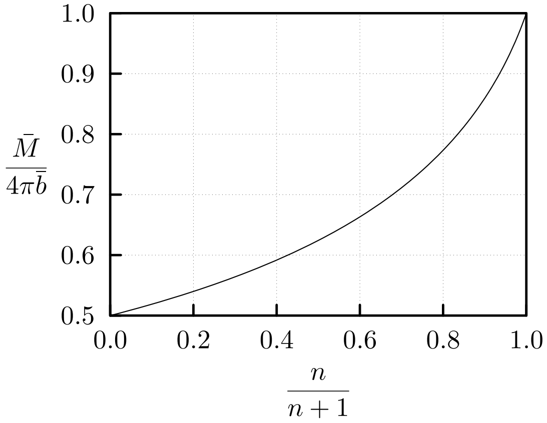

Figure 12. The dimensionless mass divided by $4\pi\bar{b}$ in the thin ring limit is plotted versus $n/(n+1)$ over the whole range of polytropic indices $n \in [0, \infty)$. The points for $n = 0$, $n = 1$ and $n \to \infty$ are known analytically and the remainder of the curve was generated by solving the equation for $\tilde{\mu}_{00}$ numerically and making use of equation (40).

Table 6. The radius ratio of the mass-shedding ring for various polytropic indices n. The value $\varrho_\mathrm{i}/\varrho_\mathrm{o} = 0$ indicates the transition from toroidal to spheroidal topologies, which only exists for $n \lesssim 0.36$.

n	0.36	1	2	3	4	5	6	7	8
$\varrho_\mathrm{i}/\varrho_\mathrm{o}$	0	0.25	0.37	0.44	0.49	0.53	0.56	0.58	0.60

demonstrate that this minimal value grows for increasing n. The value for $\varrho_\mathrm{i}/\varrho_\mathrm{o}$ at which one reaches the mass-shedding limit presumably tends to 1 as n tends to infinity. This would imply that the isothermal thin ring limit presented above and even to first order by Ostriker (1964b), i.e. in which the cross-section of the ring tends to that of a circle, is not unique. Analytic work including a family of isothermal thin ring limits and containing the mass-shedding limit will be presented elsewhere.

7 CONCLUDING REMARKS

In their work on homogeneous rings, Poincaré and Kowalewsky, whose results disagreed to first order, both had made mistakes as Dyson has shown. His result to fourth order is also erroneous as we point out in the appendix. It thus seems particularly worthwhile to test the correctness of the solutions presented here. For one thing, we ensured that the transition condition

$$\nabla U_\mathrm{in}|_\mathrm{s} = \nabla U_\mathrm{out}|_\mathrm{s} \tag{150}$$

is fulfilled up to the appropriate order in σ. Furthermore we tested that the virial theorem (49) is fulfilled for each order in σ.

Please note that one has to be careful in interpreting the results for the thin ring limit. For example, one might think that the squared angular velocity vanishes like $\sigma^2 \ln \sigma$. This is true for the dimensionless quantity $\Omega^2/G\mu_\mathrm{c}$, but need not be true for the squared angular velocity itself. If we fix the 'size' b and the mass M of the ring in that limit, then the cross-section shrinks to a point ($a = \sigma b$). With (40) we can conclude that $\mu_\mathrm{c} \propto \sigma^{-2}$ and therefore $\Omega^2 \propto \ln \sigma$, which means that Ω^2 and hence the velocity of a fluid element tend to infinity.

Relativistic rings, including the thin ring limit, were studied in Ansorg et al. (2003b), Ansorg et al. (2004) and Fischer et al. (2005). From the perspective of General Relativity, the Newtonian theory constitutes a good approximation when certain conditions are fulfilled. For one thing, typical velocities must be small compared to the speed of light c and for another $|U| \ll c^2$ must hold. We just saw, however, that for rings of finite extent and mass, the velocities grow unboundedly in the thin ring limit. The same holds for U_s as well, see (47). This means that the Newtonian theory of gravity is not appropriate to describe this subtle limit itself, since one cannot expect it to be a good approximation to General Relativity. It is remarkable that the approximation about the point $\sigma = 0$ is nevertheless so successful.

ACKNOWLEDGMENTS

It is a pleasure to thank Professor R. Meinel for fruitful discussions. The authors are also grateful to Professor J. Ostriker for pointing out his work on this subject to us. Many of the computations in this paper made use of Maple$^\mathrm{TM}$. Maple is a trademark of Waterloo Maple Inc. This research was funded in part by the Deutsche Forschungsgemeinschaft (SFB/TR7–B1).

REFERENCES

Ansorg M., Fischer T., Kleinwächter A., Meinel R., Petroff D., Schöbel K., 2004, Mon. Not. R. Astron. Soc., 355, 682
Ansorg M., Kleinwächter A., Meinel R., 2003a, Astron. Astrophys., 405, 711
Ansorg M., Kleinwächter A., Meinel R., 2003b, Astrophys. J. Lett., 582, L87
Ansorg M., Kleinwächter A., Meinel R., 2003c, Mon. Not. R. Astron. Soc., 339, 515
Ansorg M., Petroff D., 2005, Phys. Rev. D, 72, 024019
Bardeen J. M., 1971, Astrophys. J., 167, 425
Chandrasekhar S., Fermi E., 1953, Astrophys. J., 118, 116
Dyson F. W., 1892, Philos. Trans. R. Soc. London, Ser. A, 184, 43
Dyson F. W., 1893, Philos. Trans. R. Soc. London, Ser. A, 184, 1041
Eriguchi Y., Hachisu I., 1985, Astron. Astrophys., 148, 289
Eriguchi Y., Sugimoto D., 1981, Prog. Theor. Phys., 65, 1870
Fischer T., Horatschek S., Ansorg M., 2005, Mon. Not. R. Astron. Soc., 364, 943
Goenner H., 2001, Gen. Rel. Grav., 33, 833
Goenner H., Havas P., 2000, J. Math. Phys., 41, 7029
Hachisu I., 1986, Astrophys. J. Suppl. Ser., 61, 479
Kowalewsky S., 1885, Astronomische Nachrichten, 111, 37
Lichtenstein L., 1933, Gleichgewichtsfiguren rotierender Flüssigkeiten. Springer, Berlin
Ostriker J., 1964a, Astrophys. J., 140, 1056
Ostriker J., 1964b, Astrophys. J., 140, 1067
Ostriker J., 1965, Astrophys. J., 11, 167

Poincaré H., 1885a, C. R. Acad. Sci., 100, 346
Poincaré H., 1885b, Bull. Astr., 2, 109
Poincaré H., 1885c, Bull. Astr., 2, 405
Prudnikov A. P., Brychkov Y. A., Marichev O. I., 1990, Integrals and Series. Vol. 3, Gordon and Breach Science Publishers, New York
Wong C. Y., 1974, Astrophys. J., 190, 675

APPENDIX A: AN IDENTITY RELATING HYPERGEOMETRIC TO BESSEL FUNCTIONS

In order to prove the identity (141), we prove the more general identity

$$\frac{3}{40} z\, {}_2F_3\left(\frac{5}{2}, \frac{5}{2}; 3, 3, \frac{7}{2}; -z\right) - \frac{1}{2}\, {}_2F_3\left(\frac{3}{2}, \frac{3}{2}; 2, 2, \frac{5}{2}; -z\right) = \frac{\mathrm{d}}{\mathrm{d}z}\left[J_0(\sqrt{z})^2\right], \tag{A1}$$

for an arbitrary complex number z, from which (141) follows immediately.

We begin by using the differentiation properties of the hypergeometric functions, e.g. 7.2.3.47 in Prudnikov et al. (1990), to write

$$\begin{aligned}\frac{3}{40}\, {}_2F_3\left(\frac{5}{2}, \frac{5}{2}; 3, 3, \frac{7}{2}; -z\right) z - \frac{1}{2}\, {}_2F_3\left(\frac{3}{2}, \frac{3}{2}; 2, 2, \frac{5}{2}; -z\right) \\ = \frac{\mathrm{d}}{\mathrm{d}z}\Bigg[{}_2F_3\left(\frac{1}{2}, \frac{1}{2}; 1, 1, \frac{3}{2}; -z\right) \\ - \frac{z}{3}\, {}_2F_3\left(\frac{3}{2}, \frac{3}{2}; 2, 2, \frac{5}{2}; -z\right)\Bigg].\end{aligned} \tag{A2}$$

With the integral identity 7.2.3.11, the term to be differentiated can be written as

$$\begin{aligned}{}_2F_3\left(\frac{1}{2}, \frac{1}{2}; 1, 1, \frac{3}{2}; -z\right) - \frac{z}{3}\, {}_2F_3\left(\frac{3}{2}, \frac{3}{2}; 2, 2, \frac{5}{2}; -z\right) \\ = \frac{1}{\pi}\int_0^1\!\!\int_0^1 \frac{J_0(2\sqrt{t_1 t_2 z})}{2\sqrt{t_1 t_2 (1-t_1)}} - \frac{z J_1(2\sqrt{t_1 t_2 z})}{2\sqrt{z(1-t_1)}}\, \mathrm{d}t_1\, \mathrm{d}t_2,\end{aligned} \tag{A3}$$

where we have made use of the identity (e.g. 7.13.1.1 in Prudnikov et al. 1990)

$${}_0F_1(b, -z) = \Gamma(b) z^{(1-b)/2} J_{b-1}(2\sqrt{z}). \tag{A4}$$

The above double integral yields

$$\begin{aligned}\frac{1}{\pi}\int_0^1\!\!\int_0^1 \frac{J_0(2\sqrt{t_1 t_2 z})}{2\sqrt{t_1 t_2 (1-t_1)}} - \frac{z J_1(2\sqrt{t_1 t_2 z})}{2\sqrt{z(1-t_1)}}\, \mathrm{d}t_1\, \mathrm{d}t_2 \\ = \frac{1}{\pi}\int_0^1 \frac{J_0(2\sqrt{t_1 z})}{t_1(1-t_1)} \mathrm{d}t_1 = J_0(\sqrt{z})^2,\end{aligned} \tag{A5}$$

thereby proving (A1).

APPENDIX B: FURTHER COEFFICIENTS

In Tables B1–B4, coefficients for Ω_i, β_{ik}, $U_{ik}(y)$ and α_{li} for homogeneous rings are given.

Table B1. Coefficients Ω_i for homogeneous rings up to the order $q = 9$ ($i = 2, 3, \ldots, 10$).

i	Ω_i
2	$\lambda + \frac{3}{4}$
3	0
4	$-\frac{1}{8}\,\lambda - \frac{19}{96}$
5	0
6	$\frac{25}{128}\,\lambda^3 + \frac{365}{1536}\,\lambda^2 - \frac{2345}{18432}\,\lambda - \frac{8989}{73728}$
7	0
8	$\frac{25}{64}\,\lambda^4 + \frac{40235}{98304}\,\lambda^3 - \frac{134255}{294912}\,\lambda^2 - \frac{36493505}{56623104}\,\lambda - \frac{34831813}{226492416}$
9	0
10	$\frac{134925}{131072}\,\lambda^5 + \frac{2797535}{1572864}\,\lambda^4 - \frac{50072105}{169869312}\,\lambda^3 -$ $\frac{1021727845}{509607936}\,\lambda^2 - \frac{104581877693}{97844723712}\,\lambda - \frac{49377918425}{391378894848}$

Table B2. Coefficients β_{ik} for homogeneous rings up to the order $q = 9$. The bold-faced type indicates that these terms are incorrect in Dyson (1892).

$_i\diagdown^k$	1	2	3	4	5	6	7	8	9
1	0	—	—	—	—	—	—	—	—
2	0	$\frac{5}{8}\lambda + \frac{35}{96}$	—	—	—	—	—	—	—
3	0	0	$\frac{5}{128}\lambda - \frac{35}{3072}$	—	—	—	—	—	—
4	0	$\frac{5}{8}\lambda^2 + \boldsymbol{\frac{95}{128}}\lambda + \boldsymbol{\frac{1145}{9216}}$	0	$\frac{75}{256}\lambda^2 + \boldsymbol{\frac{815}{2304}}\lambda + \boldsymbol{\frac{5089}{55296}}$	—	—	—	—	—
5	$-\frac{25}{1024}\lambda^2 - \frac{175}{24576}\lambda + \frac{1225}{294912}$	0	$\frac{15}{256}\lambda^2 + \frac{4955}{147456}\lambda - \frac{62141}{3538944}$	0	$\frac{25}{512}\lambda^2 + \frac{75}{4096}\lambda - \frac{14455}{1179648}$	—	—	—	—
6	0	$\frac{5185}{4096}\lambda^3 + \frac{110515}{49152}\lambda^2 + \frac{853225}{884736}\lambda + \frac{34487}{1327104}$	0	$\frac{75}{128}\lambda^3 + \frac{116545}{110592}\lambda^2 + \frac{308395}{589824}\lambda + \frac{17892169}{318504960}$	0	$\frac{625}{4096}\lambda^3 + \frac{169625}{589824}\lambda^2 + \frac{1097461}{7077888}\lambda + \frac{7327349}{339738624}$	—	—	—
7	$-\frac{125}{2048}\lambda^3 - \frac{76325}{1179648}\lambda^2 + \frac{78175}{28311552}\lambda + \frac{1313095}{169869312}$	0	$\frac{1325}{8192}\lambda^3 + \frac{109915}{442368}\lambda^2 + \frac{863633}{18874368}\lambda - \frac{105833029}{4076863488}$	0	$\frac{125}{1024}\lambda^3 + \frac{9815}{73728}\lambda^2 - \frac{472843}{56623104}\lambda - \frac{32985941}{1509949440}$	0	$\frac{375}{8192}\lambda^3 + \frac{4825}{98304}\lambda^2 - \frac{34745}{9437184}\lambda - \frac{268795}{28311552}$	—	—
8	0	$\frac{11935}{4096}\lambda^4 + \frac{15693265}{2359296}\lambda^3 + \frac{387327415}{84934656}\lambda^2 + \frac{1967050099}{2717908992}\lambda - \frac{21240691225}{195689447424}$	0	$\frac{48175}{32768}\lambda^4 + \frac{299613275}{84934656}\lambda^3 + \frac{86354441}{31850496}\lambda^2 + \frac{163195481003}{244611809280}\lambda + \frac{61946667647}{14676708556800}$	0	$\frac{1875}{4096}\lambda^4 + \frac{1994875}{1769472}\lambda^3 + \frac{1544984219}{1698693120}\lambda^2 + \frac{26196760631}{101921587200}\lambda + \frac{523810097561}{34245653299200}$	0	$\frac{21875}{262144}\lambda^4 + \frac{2069375}{9437184}\lambda^3 + \frac{7862435}{42467328}\lambda^2 + \frac{6142108445}{114152177664}\lambda + \frac{968695327}{342456532992}$	—
9	$-\frac{26875}{131072}\lambda^4 - \frac{10803575}{28311552}\lambda^3 - \frac{73205885}{452984832}\lambda^2 + \frac{245384393}{10871635968}\lambda + \frac{5148689159}{391378894848}$	0	$\frac{58565}{131072}\lambda^4 + \frac{317810795}{339738624}\lambda^3 + \frac{4061560685}{8153726976}\lambda^2 - \frac{3261000013}{97844723712}\lambda - \frac{1033257753043}{23482733690880}$	0	$\frac{3125}{8192}\lambda^4 + \frac{20750915}{28311552}\lambda^3 + \frac{738672683}{2264924160}\lambda^2 - \frac{180456831247}{3261490790400}\lambda - \frac{13297677452861}{365286968524800}$	0	$\frac{2625}{16384}\lambda^4 + \frac{2597725}{9437184}\lambda^3 + \frac{112005563}{1358954496}\lambda^2 - \frac{117378627479}{2283043553280}\lambda - \frac{173703027451}{9132174213120}$	0	$\frac{625}{16384}\lambda^4 + \frac{72125}{1048576}\lambda^3 + \frac{4955105}{226492416}\lambda^2 - \frac{79046365}{5435817984}\lambda - \frac{1636799939}{260919263232}$

Table B3. Coefficients $U_{ik}(y)$ for homogeneous rings up to the order $q = 7$.

$i \backslash k$	0	1	2	3	4	5	6	7
0	$2\,\lambda + 5 - y^2$	—	—	—	—	—	—	—
1	0	$(\lambda + 1)y - \frac{1}{4}\,y^3$	—	—	—	—	—	—
2	$-\frac{1}{8}\,\lambda - \frac{7}{32} + (\frac{1}{4}\,\lambda + \frac{1}{4})y^2 - \frac{3}{32}\,y^4$	0	$(\lambda + \frac{31}{48})y^2 - \frac{5}{48}\,y^4$	—	—	—	—	—
3	0	$(-\frac{13}{32}\,\lambda - \frac{65}{192})y + (\frac{7}{16}\,\lambda + \frac{67}{192})y^3 - \frac{15}{128}\,y^5$	0	$(\frac{15}{64}\,\lambda + \frac{175}{1536})y^3 - \frac{35}{768}\,y^5$	—	—	—	—
4	$\frac{25}{64}\,\lambda^3 + \frac{295}{384}\,\lambda^2 + \frac{3457}{9216}\,\lambda + \frac{19}{576} + (-\frac{13}{128}\,\lambda - \frac{65}{768})y^2 + (\frac{21}{128}\,\lambda + \frac{67}{512})y^4 - \frac{25}{512}\,y^6$	0	$(\frac{5}{8}\,\lambda^2 + \frac{311}{512}\,\lambda + \frac{269}{36864})y^2 + (\frac{185}{768}\,\lambda + \frac{3205}{18432})y^4 - \frac{35}{512}\,y^6$	0	$(\frac{455}{4608}\,\lambda + \frac{4459}{110592})y^4 - \frac{21}{1024}\,y^6$	—	—	—
5	0	$(\frac{25}{128}\,\lambda^3 - \frac{355}{1536}\,\lambda^2 - \frac{20005}{36864}\,\lambda - \frac{11081}{73728})y + (\frac{5}{32}\,\lambda^2 + \frac{155}{2048}\,\lambda - \frac{9091}{147456})y^3 + (\frac{465}{2048}\,\lambda + \frac{2855}{16384})y^5 - \frac{875}{12288}\,y^7$	0	$(\frac{15}{256}\,\lambda^2 + \frac{25}{73728}\,\lambda - \frac{100015}{1769472})y^3 + (\frac{4795}{36864}\,\lambda + \frac{76223}{884736})y^5 - \frac{315}{8192}\,y^7$	0	$(\frac{805}{18432}\,\lambda + \frac{26579}{1769472})y^5 - \frac{77}{8192}\,y^7$	—	—
6	$\frac{25}{32}\,\lambda^4 + \frac{95435}{49152}\,\lambda^3 + \frac{862135}{589824}\,\lambda^2 + \frac{7959115}{28311552}\,\lambda - \frac{551045}{28311552} + (\frac{25}{512}\,\lambda^3 - \frac{355}{6144}\,\lambda^2 - \frac{20005}{147456}\,\lambda - \frac{11081}{294912})y^2 + (\frac{15}{256}\,\lambda^2 + \frac{465}{16384}\,\lambda - \frac{9091}{393216})y^4 + (\frac{775}{8192}\,\lambda + \frac{14275}{196608})y^6 - \frac{6125}{196608}\,y^8$	0	$(\frac{335}{256}\,\lambda^3 + \frac{9895}{4608}\,\lambda^2 + \frac{440125}{589824}\,\lambda - \frac{1755973}{42467328})y^2 + (\frac{245}{3072}\,\lambda^2 + \frac{9325}{294912}\,\lambda - \frac{31315}{786432})y^4 + (\frac{455}{3072}\,\lambda + \frac{32011}{294912})y^6 - \frac{1575}{32768}\,y^8$	0	$(\frac{125}{6912}\,\lambda^2 - \frac{2765}{1769472}\,\lambda - \frac{1824697}{79626240})y^4 + (\frac{10241}{147456}\,\lambda + \frac{1504909}{35389440})y^6 - \frac{693}{32768}\,y^8$	0	$(\frac{17549}{884736}\,\lambda + \frac{243479}{42467328})y^6 - \frac{143}{32768}\,y^8$	—
7	0	$(\frac{25}{64}\,\lambda^4 - \frac{40645}{98304}\,\lambda^3 - \frac{2042065}{1179648}\,\lambda^2 - \frac{58120985}{56623104}\,\lambda - \frac{39130979}{339738624})y + (\frac{745}{2048}\,\lambda^3 + \frac{36385}{73728}\,\lambda^2 + \frac{200065}{2359296}\,\lambda - \frac{6542965}{169869312})y^3 + (\frac{645}{8192}\,\lambda^2 + \frac{27925}{786432}\,\lambda - \frac{645475}{18874368})y^5 + (\frac{85225}{589824}\,\lambda + \frac{1539545}{14155776})y^7 - \frac{25725}{524288}\,y^9$	0	$(\frac{1485}{8192}\,\lambda^3 + \frac{439675}{1769472}\,\lambda^2 - \frac{246977}{28311552}\,\lambda - \frac{513938083}{10192158720})y^3 + (\frac{17435}{442368}\,\lambda^2 + \frac{190295}{14155776}\,\lambda - \frac{117973177}{5096079360})y^5 + (\frac{36449}{393216}\,\lambda + \frac{6114493}{94371840})y^7 - \frac{8085}{262144}\,y^9$	0	$(\frac{12385}{1769472}\,\lambda^2 + \frac{35497}{28311552}\,\lambda - \frac{181782779}{20384317440})y^5 + (\frac{5425}{147456}\,\lambda + \frac{2961899}{141557760})y^7 - \frac{3003}{262144}\,y^9$	0	$(\frac{32417}{3538944}\,\lambda + \frac{375383}{169869312})y^7 - \frac{2145}{1048576}\,y^9$

Table B4. Coefficients α_{li} for homogeneous rings up to the order $q = 8$.

$l \backslash i$	0	1	2	3	4	5	6	7	8
1	1	0	0	0	$\frac{25}{128}\lambda^2 + \frac{175}{768}\lambda + \frac{1225}{18432}$	0	$\frac{25}{64}\lambda^3 + \frac{68075}{98304}\lambda^2 + \frac{410275}{1179648}\lambda + \frac{2568475}{56623104}$	0	$\frac{134925}{131072}\lambda^4 + \frac{239525}{98304}\lambda^3 + \frac{316929175}{169869312}\lambda^2 + \frac{1001961695}{2038431744}\lambda + \frac{2116102111}{97844723712}$
2	—	$-\frac{1}{8}$	0	$-\frac{25}{32}\lambda - \frac{175}{384}$	0	$-\frac{475}{512}\lambda^2 - \frac{555}{512}\lambda - \frac{965}{4608}$	0	$-\frac{10025}{4096}\lambda^3 - \frac{1698785}{393216}\lambda^2 - \frac{28823195}{14155776}\lambda - \frac{123632507}{679477248}$	0
3	—	—	$\frac{5}{16}\lambda + \frac{17}{96}$	0	$\frac{5}{16}\lambda^2 + \frac{1315}{3072}\lambda + \frac{9235}{73728}$	0	$\frac{1765}{2048}\lambda^3 + \frac{1985}{1024}\lambda^2 + \frac{4356505}{3538944}\lambda + \frac{18119345}{84934656}$	0	$\frac{2195}{1024}\lambda^4 + \frac{3052455}{524288}\lambda^3 + \frac{888829145}{169869312}\lambda^2 + \frac{515947105}{301989888}\lambda + \frac{13524934807}{97844723712}$
4	—	—	—	$-\frac{5}{256}\lambda - \frac{107}{6144}$	0	$-\frac{475}{1536}\lambda^2 - \frac{323095}{884736}\lambda - \frac{2199527}{21233664}$	0	$-\frac{15815}{24576}\lambda^3 - \frac{6138925}{5308416}\lambda^2 - \frac{71128549}{113246208}\lambda - \frac{12275264429}{122305904640}$	0
5	—	—	—	—	$\frac{25}{768}\lambda^2 + \frac{515}{13824}\lambda + \frac{13777}{1327104}$	0	$\frac{25}{384}\lambda^3 + \frac{163145}{1327104}\lambda^2 + \frac{62041}{786432}\lambda + \frac{133449991}{7644119040}$	0	$\frac{20225}{98304}\lambda^4 + \frac{81963095}{127401984}\lambda^3 + \frac{260962627}{382205952}\lambda^2 + \frac{10908318845}{36691771392}\lambda + \frac{1946363428441}{44030125670400}$
6	—	—	—	—	—	$-\frac{25}{24576}\lambda^2 - \frac{3749}{1769472}\lambda - \frac{384013}{424673280}$	0	$-\frac{425}{12288}\lambda^3 - \frac{5290135}{84934656}\lambda^2 - \frac{82443283}{2264924160}\lambda - \frac{6684148507}{978447237120}$	0
7	—	—	—	—	—	—	$\frac{125}{73728}\lambda^3 + \frac{20765}{7077888}\lambda^2 + \frac{77707}{47185920}\lambda + \frac{6177187}{20384317440}$	0	$\frac{125}{24576}\lambda^4 + \frac{515945}{42467328}\lambda^3 + \frac{1166591837}{101921587200}\lambda^2 + \frac{62067170651}{12230590464000}\lambda + \frac{3643667826661}{4109478395904000}$
8	—	—	—	—	—	—	—	$-\frac{25}{1179648}\lambda^3 - \frac{595}{6291456}\lambda^2 - \frac{619081}{6794772480}\lambda - \frac{28211731}{1141521776640}$	0
9	—	—	—	—	—	—	—	—	$\frac{125}{2359296}\lambda^4 + \frac{41825}{339738624}\lambda^3 + \frac{1276387}{12230590464}\lambda^2 + \frac{692812541}{17978967982080}\lambda + \frac{18307106611}{3451961852559360}$